AD-768 161

RESPONSE OF LEAD AZIDE TO SPARK DISCHARGES VIA A NEW PARALLEL-PLATE ELECTROSTATIC SENSITIVITY APPARATUS

Maurice S. Kirshenbaum

Picatinny Arsenal
Dover, New Jersey

June 1973

DISTRIBUTED BY:

NTIS
National Technical Information Service
U. S. DEPARTMENT OF COMMERCE
5285 Port Royal Road, Springfield Va. 22151

UNCLASSIFIED
Security Classification

DOCUMENT CONTROL DATA - R & D

(Security classification of title, body of abstract and indexing annotation must be entered when the overall report is classified)

1. ORIGINATING ACTIVITY *(Corporate author)* Picatinny Arsenal, Dover, New Jersey 07801	2a. REPORT SECURITY CLASSIFICATION Unclassified 2b. GROUP

3. REPORT TITLE

Response of Lead Azide to Spark Discharges Via a New Parallel-Plate Electrostatic Sensitivity Apparatus

4. DESCRIPTIVE NOTES *(Type of report and inclusive dates)*

5. AUTHOR(S) *(First name, middle initial, last name)*

M.S. Kirshenbaum

6. REPORT DATE June 1973	7a. TOTAL NO. OF PAGES ~~90~~ 94	7b. NO. OF REFS 15
8a. CONTRACT OR GRANT NO. b. PROJECT NO. c. AMCMS Code 662603.11.55901 d.	9a. ORIGINATOR'S REPORT NUMBER(S) Technical Report 4559 9b. OTHER REPORT NO(S) *(Any other numbers that may be assigned this report)*	

10. DISTRIBUTION STATEMENT

Distribution of this document is unlimited.

11. SUPPLEMENTARY NOTES	12. SPONSORING MILITARY ACTIVITY Picatinny Arsenal, Dover, N. J.

13. ABSTRACT

The report describes a fixed-gap, spark discharge apparatus having parallel-plate electrodes, and instrumentation for measuring time-dependent spark characteristics. The response of lead azide (RD 1333) to gaseous spark discharge as a function of the electrode geometry and of the properties of the discharge circuit was studied. A method for measuring the energy in the spark gap is described. A computer program was developed for reducing the data from the observed current and voltage waveforms to current, voltage, power and energy in the gap and for plotting these values as a function of time.

Results show that the initiation of lead azide by gaseous discharge is not entirely dependent on the energy dissipated in the spark gap, but is a strong function of the electrode geometry, the circuit storage capacitance, and series resistance, particularly as they affect the energy delivery rate to the spark gap. A comparison with the fixed-gap, needle-to-plane test method showed that the parallel-plate configuration resulted in lower, more reproducible minimum initiation energies, and therefore a better hazard evaluation. The need is discussed for a versatile electrostatic sensitivity apparatus and a test method for evaluating hazardous situations.

Reproduced by
NATIONAL TECHNICAL
INFORMATION SERVICE
U S Department of Commerce
Springfield VA 22151

DD FORM 1 NOV 65 1473 REPLACES DD FORM 1473, 1 JAN 64, WHICH IS OBSOLETE FOR ARMY USE.

UNCLASSIFIED
Security Classification

UNCLASSIFIED
Security Classification

KEY WORDS	LINK A ROLE	LINK A WT	LINK B ROLE	LINK B WT	LINK C ROLE	LINK C WT
Electrostatic Spark Sensitivity of Primary Explosives						
Lead Azide						
Lead Styphnate						
Fixed Spark Gap Discharge Apparatus						
Parallel-Plate Electrodes						
Needle-Plane Electrodes						
Spark (Discharge)						
Gaseous Discharge						
Condenser Discharge						
Current and Voltage Waveforms						
Energy Dissipation in the Spark Gap						
Electrostatic Hazards						

UNCLASSIFIED
Security Classification

AD-768161

Technical Report 4559

Response of Lead Azide to Spark Discharges Via a New Parallel-Plate Electrostatic Sensitivity Apparatus

by

Maurice S. Kirshenbaum

June 1973

Approved for public release; distribution unlimited
AMCMS Code 662603.11.55901

Explosives Division
Feltman Research Laboratory
Picatinny Arsenal
Dover, New Jersey

The citation in this report of the trade names of commercially available products does not constitute official indorsement or approval of the use of such products.

TABLE OF CONTENTS

	Page No.
Abstract	1
Introduction	2
Experimental	5
Apparatus	5
Materials	5
Procedure	5
Results	11
Spark Discharge Characteristics	11
Reproducibility	12
Energy Response Curve	13
Energy in the Spark Gap	16
The Effect of Energy Delivery Rate on the Initiation of Lead Azide (BD 1333)	19
Needle-Plane Electrodes	30
Discussion	31
Rate Effect	31
Initiation Mechanism	33
Safety	33
Gap Breakdown	35
Electrode Geometry	37
Conclusions	39
Future Work	41
Acknowledgements	43
References	44
Appendices	46
A. Description of Apparatus	46
B. Spark Discharge Characteristics	53
C. Energy Determination	66
Distribution List	86

TABLE OF CONTENTS (Continued)

		Page No.
Tables		
1	Reproducibility Test Results for the Electrostatic Sensitivity Apparatus	14
2	The Effect of Series Resistance on the Initiation of Lead Azide (RD 1333)	21
3	The Effect of Capacitance on the Initiation of Lead Azide (RD 1333)	23
4	50 Percent Initiation Points	29
5	Comparison of the Minimum Initiation Energy of Lead Azide (RD 1333) Obtained by the Needle-Plane Electrodes and the Parallel-Plate Electrodes	32
6	Dependence of Spark Duration on Series Resistance and Capacitance	60
Figures		
1	Parallel-Plate Electrode Apparatus	6
2	Needle-Plane Electrode Apparatus	7
3	Lead Azide Energy Response Curve	15
4	Energy Dissipated in Spark Gap as a Function of the Series Resistance: Mercury Switch	17
5	Energy Dissipated in Spark Gap as a Function of the Series Resistance: Krytron Switch	18
6	The Effect of Energy Delivery Rate on the Initiation of Lead Azide: 50 Percent Firing Points	22
7	The Effect of Capacitance on Initiation of Lead Azide: Minimum Energy	25

TABLE OF CONTENTS (Continued)

		Page No.
Figures (Continued)		
8	The Effect of RC Time Constant on Initiation of Lead Azide: Minimum Energy	26
9	No Gap Breakdown	28
10	Lead Azide After Spark Discharge: No Detonation	38
11	Low Voltage Circuit	47
12	High Voltage Circuit	49
13a	Parallel-Plate Electrode Assembly: Photo	50
13b	Parallel-Plate Electrode Assembly: Schematic	51
14	Needle Assembly	54
15	Typical Oscilloscope Traces of Voltage and Current During Spark Discharge with Mercury Switch: 1800 pF Capacitance	56
16	Typical Voltage and Current Characteristics of a Spark with Mercury Switch: 3500 pF Capacitance	61
17	Typical Voltage and Current Characteristics of a Spark with Krytron Switch: 1800 pF Capacitance	62
18	Typical Oscilloscope Traces of Voltage Across Spark Gap and Series Resistance During Discharge with Krytron Switch: 1000 pF Capacitance	64
19	Relaxation Oscillation Discharge	65

ABSTRACT

The report describes a fixed-gap, spark discharge apparatus having parallel-plate electrodes, and instrumentation for measuring time-dependent spark characteristics. The response of lead azide (RD 1333) to gaseous spark discharge as a function of the electrode geometry and of the properties of the discharge circuit is presented. A method for measuring the energy in the spark gap is described. A computer program was developed for reducing the data from the observed current and voltage waveforms to current, voltage, power and energy in the gap and for plotting these values as a function of time.

Results show that the initiation of lead azide by gaseous discharge is not entirely dependent on the energy dissipated in the spark gap, but is a strong function of the electrode geometry, the circuit storage capacitance, and series resistance, particularly as they affect the energy delivery rate to the spark gap. A comparison with the fixed-gap, needle-to-plane test method showed that the parallel-plate configuration resulted in lower, more reproducible minimum initiation energies, and therefore a better hazard evaluation. The need is discussed for a versatile electrostatic sensitivity apparatus and a test method for evaluating hazardous situations.

INTRODUCTION

This study was undertaken to improve electrostatic sensitivity tests and to assess the relative electrostatic hazards of several competing proposals to automate the primary explosives process line in munitions plants.

Electrostatic sensitivity tests are used by the explosives munitions industry to assess the electrostatic hazards associated with the processing and handling of explosives. In these tests, a charged capacitor is discharged through a spark gap in or near the explosive and a threshold or a minimum spark energy capable of initiating the explosive is usually determined. Widely varying minimum energy values are obtained for the same explosive when different experimental apparatus or conditions are used. It is possible for the ranking of the sensitivities of explosives to vary from one apparatus to another.

Some of the differences among various types of test apparatus and procedures have been explained by Moore, Sumner and Wyatt [illegible]. They have shown that the electrical circuit, spark gap-explosive geometry, ambient conditions, and the nature of the explosive all play important roles. The circuit components and spark gap geometry can affect the rate of energy delivery, the efficiency of energy transfer, and the character of the spark. One of the problems in electrostatic sensitivity testing is the differentiation between the contributions of the spark and those of the explosive to the observed

results. For example, an electrostatic sensitivity apparatus which uses a large capacitance may yield minimum energies for initiation which are related only to the threshold for gap breakdown and not to the sensitivity of the explosive. Other important questions relate to the reproducibility of the tests; effects of energy delivery rate, ambient conditions, electrode geometry, and characteristics of the explosive (purity, density, and particle size distribution) on initiation probability; and the testing methodology that yields a minimum energy most meaningful for a hazards analysis. This report attempts to answer some of these questions.

The electrostatic hazards involved in the plant operations and in any processing line can be predicted only by considering the following:

(a) The generat on, transport, build-up and relaxation of the electrostatic charges produced in handling and processing explosives.

(b) A mechanism for the transfer of the stored charge or energy to an electrostatic discharge.

(c) The type of discharge obtained (contact or spark).

(d) The transfer of energy into the explosive.

(e) The minimum spark energy capable of initiating the primary explosives.

To satisfy the two goals described (better electrostatic sensitivity testing and improvement of manufacturing technology), the following objectives were adopted for the electrostatic hazards program:

(a) The development of a versatile electrostatic sensitivity apparatus and testing procedure which are safe, convenient and capable of yielding reproducible results.

(b) The determination of the current and voltage characteristics of the spark, of the energy delivery rate, and of the energy delivered to the spark gap for gaseous discharge as functions of the test parameters.

(c) The determination of the effect of the energy delivery rate on the initiation probability.

(d) The determination of the minimum initiation energy most meaningful for a hazard analysis using gaseous discharge and lead azide (RD 1333) as a sample substance.

The work described is part of an effort to advance the level of competence with respect to electrostatic hazards analysis. This effort has already produced the following contributions: the quantitative description and hazards analysis of electrostatic charge generation in a solid-fluid system during filtration and washing processes[8]; the characterization of the charging and discharging mechanisms in dry primary explosive powders[9]; the review of existing electrostatic testing methods and techniques and a critique of the spark initiation tests used at both Picatinny Arsenal and the Naval Ordnance Laboratory[10].

EXPERIMENTAL

Apparatus

A fixed-gap, parallel-plate configuration was selected for the design of the electrostatic spark discharge apparatus because it was found that this configuration allows better control over the spark-explosive geometry and minimizes corona losses. The apparatus was designed to be simple and safe, and to give reproducible results. The first model (Figures 1 and 2) was also versatile enough in design to allow it to be used in an extensive research program using either parallel-plate or needle-plane electrodes. It consisted of a variable high voltage power supply; an electrical charging circuit; a triggering circuit; an electrostatic voltmeter; a fixed gap electrode assembly (the gap could be varied and measured as required); and a high speed dual beam oscilloscope. A detailed description of the apparatus is contained in Appendix A.

Materials

Lead azide (RD 1333) DuPont Lot Number 51-49, was used for the investigation. The explosive powder was stored in closed containers and was preconditioned by storage in the test room at 30 to 45 percent relative humidity for at least 24 hours prior to test.

Procedures

Parallel-Plate Geometry

The selected capacitance and resistance were connected in the firing circuit. Samples varying in weight from six to eight

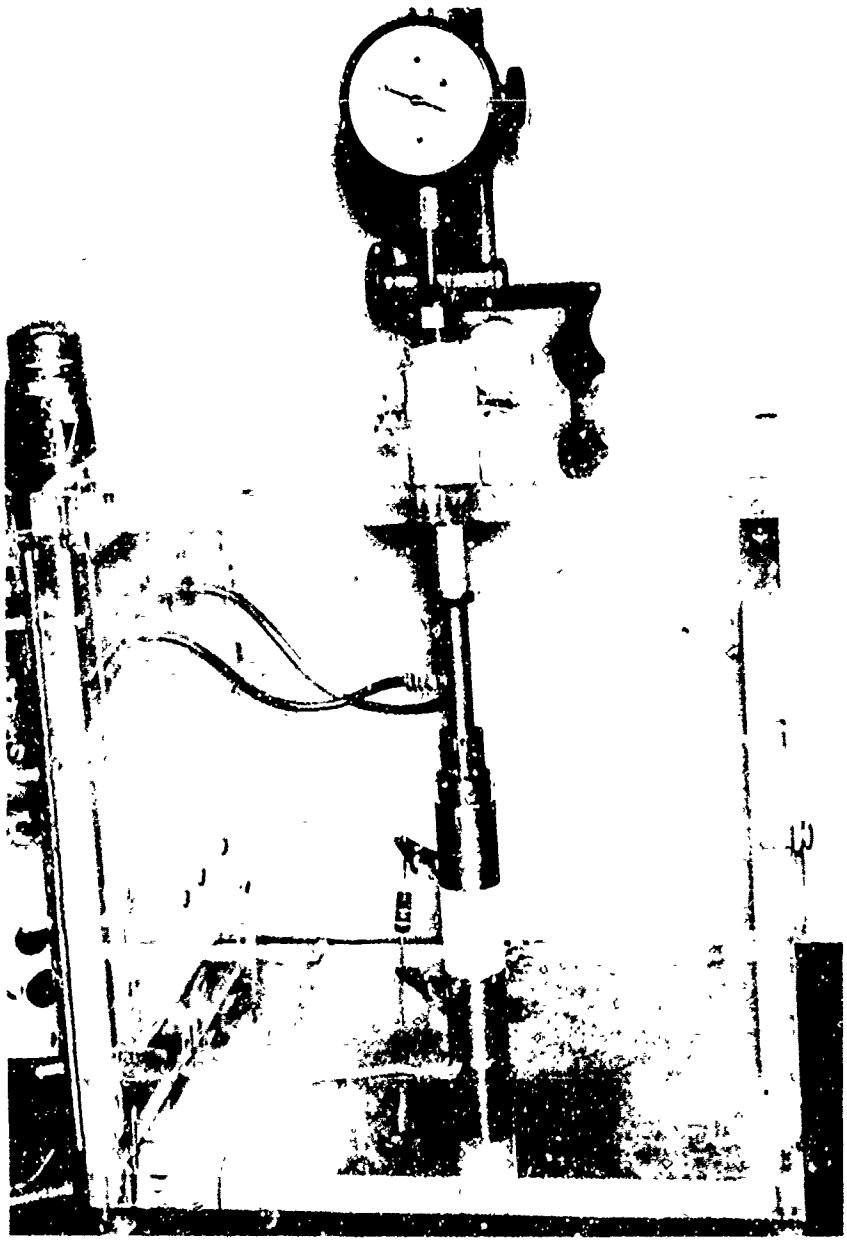

PARALLEL-PLATE ELECTRODE APPARATUS

FIGURE 1

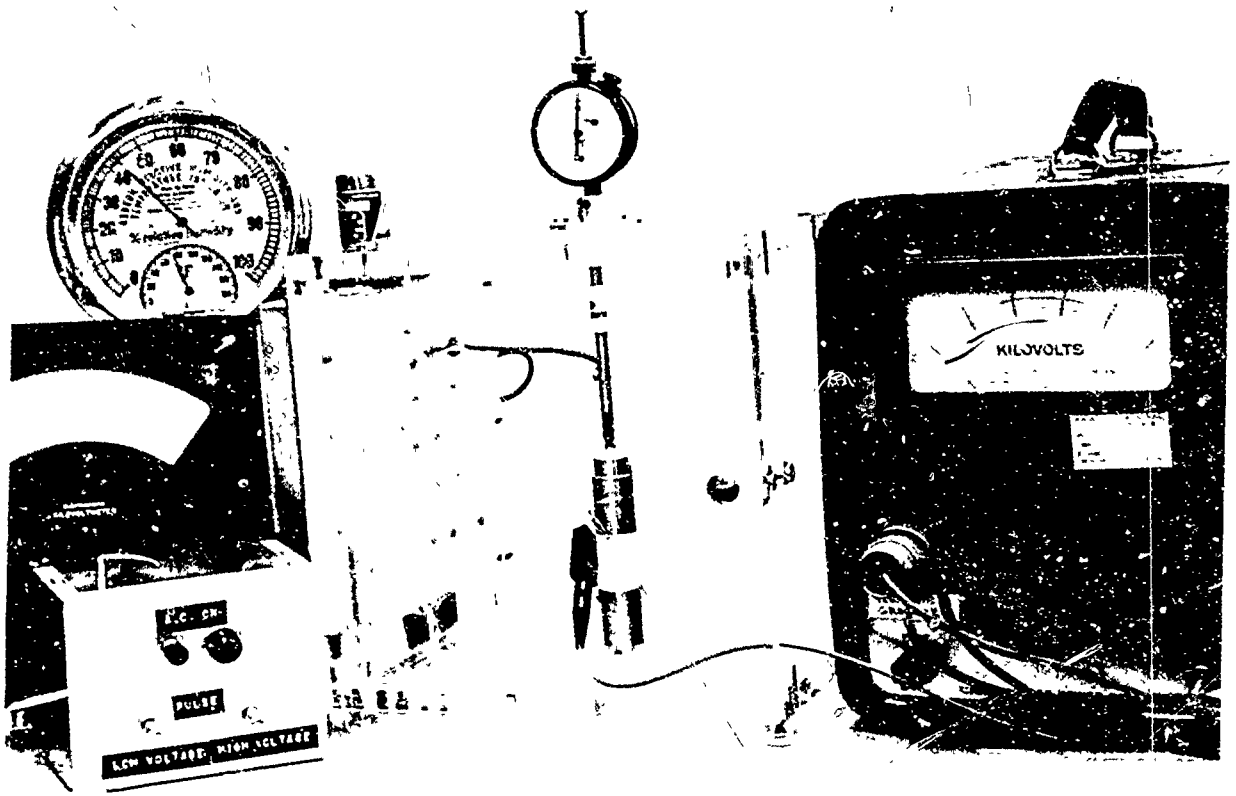

NEEDLE-PLANE ELECTRODE APPARATUS

FIGURE 2

milligrams were used in the tests. It was noted during the reproducibility tests that these weight variations had little influence on the initiation energies. The explosive powder was placed in the sample holder consisting of a 3/16-inch diameter hole in a disc of a 0.0075-inch-thick polyvinyl chloride electrical tape on a 3/4-inch-diameter flat steel disc. The sample holder, after being tapped gently so that the powder completely covered the bottom and distributed itself evenly across the hole, was placed on the base electrode. The upper electrode was lowered to the appropriate gap distance, the thickness of the electrical tape, 0.0075 inch. Thus, the explosive powder loosely filled the gap; the spark discharge occurred through the interstices of the powder. Throughout this series of tests the gap setting, which was read on the dial indicator, was kept constant. The storage capacitor was charged to the desired voltage, which was read on the electrostatic voltmeter.

The test was initiated by activating a relay with mercury wetted contacts for tests below 1000 volts and a Krytron switch for voltages up to 5000 volts. Most of the potential of the capacitor was developed across the series resistance and the sample spark gap although some energy was lost in the switch. Initiation or non-initiation of the explosive was observed. The spark voltage and current oscilloscope traces were recorded photographically to determine the energy delivered to the sample. Internal triggering of the oscilloscope from the current pulse was used in making these records. After each trial,

a fresh sample was used, whether or not initiation had occurred. A total of 25 trials were carried out at each set of test conditions, except when determining the minimum energy. For the latter, the test parameters were changed after either an initiation or the completion of 25 trials, whichever came first. After each initiation, the electrodes were cleaned with No. 400 and No. 600 emery cloth and polished with crocus cloth to remove the lead deposit.

Point-to-Plane Geometry

A procedure similar to the one used for the parallel-plate configuration was used for the needle-plane geometry. A 6-8 mg explosive sample was placed on the steel sample holder which, in turn, was placed on the base electrode. During routine tests, it was noted that the sample size in this weight range had little influence on sensitivity. The needle electrode (upper) was lowered to the desired gap length, usually 0.005 inch, so that the point of the needle was buried in the powder. A gap of 0.005 inch was used because it was difficult to obtain a spark discharge for a 0.0075 inch gap in the absence of powder at the maximum voltage. In addition, Moore, Sumner, and Wyatt[2] indicated that the 0.005 inch gap was optimum for energy transfer for the needle-plane electrodes. The storage capacitor was charged to the desired voltage and was allowed to discharge through the powder by activating the Krytron switch.

Several trials were carried out on each sample of explosive on the sample holder if initiation did not occur in order to increase

the number of tests conducted in a day. However, a different portion of the sample was exposed to each discharge by moving the holder about on the base electrode. After each explosive initiation, the sample holder was cleaned and the phonograph needle replaced. It should be noted that for the parallel-plate configuration fresh explosive powder was used for each trial because with this configuration it was impossible to expose a different portion of the explosive sample to each discharge.

Minimum Initiation Energy Determination

A series of initiation tests, using a range of capacitances and resistances, was carried out in an attempt to determine a meaningful minimum energy. The capacitances used were 250, 500, 1000, 2000 and 3000 pF. The values of the resistances were 0.15, 82, 1K, 10K, 100K, 680K and 1.2M ohms. The appropriate capacitance and resistance were placed in the firing circuit. The starting point was an arbitrary one, usually the largest capacitor and resistor, unless a more efficient value based on experience was known. The energy of the spark was reduced in increments by decreasing the voltage across the capacitor until no initiation was obtained in 25 consecutive trials. Then the resistance was changed to the next lower value and the procedure repeated, using the voltage setting which yielded the lowest energy in the previous test as the new starting point. This procedure was continued until the lowest delivered energy for a specific capacitance was attained. Then a second set of trials was carried out with the

next capacitor, usually one having half the capacitance of the previous capacitor. This procedure was repeated until a minimum was noted or all capacitors were used.

RESULTS

Spark Discharge Characteristics

A series of experiments was carried out to characterize the spark discharge in air for the fixed-gap, parallel-plate, electrode apparatus as a function of the capacitance and resistance in the spark discharge circuit. These experiments showed that, when a charged capacitor was discharged by a mercury switch through the spark gap with no added series resistance, the current and voltage varied in an oscillatory manner due to a 0.55μH stray inductance in the circuit. The current and voltage were slightly out of phase, the voltage leading the current. When a KN-22 Krytron switch was substituted for the mercury switch, oscillatory discharges were not obtained since the Krytron provided some rectification of the current.

The addition of series resistances to the discharge circuit had a tworold effect. First, the character of the discharge changed from oscillatory to unidirectional. With large series resistances, hundreds of kilohms, the discharge was no longer continuous but took the form of a series of burst of sparks due to relaxation oscillations. In addition to changing the character of the discharge, series resistance also changed the duration of the spark. The effective spark

duration decreased to a minimum with about 20 ohms and then gradually increased with further increase of resistance. The second effect of adding resistance was to reduce the fraction of the energy in the capacitor that was actually delivered to the spark gap. This energy decreased from approximately 80 percent to 10 to 14 percent as the series resistance was increased from zero to 1000 ohms and then remained practically constant at the 10 to 14 percent level as the resistance was further increased. This second effect is discussed in more detail in another section of the report (Energy in the Spark Gap). Increasing the capacitance in the circuit increased the duration of the discharge as well as increasing the energy available across the sparkgap. The spark discharge characteristics are treated in detail in Appendix B.

Reproducibility

Before carrying out experiments to determine the effect of the energy delivery rate on the initiation probability of lead azide (RD 1333), it was necessary to determine the reproducibility of the apparatus. Two series of tests were conducted. The results, summarized in Table 1, show excellent reproducibility.

The first series was carried out at approximately the 30 percent firing point for lead azide. The firing circuit contained three nominal 1000-pF capacitors in parallel (2850 pF measured capacitance) charged to 4000 volts, a 56-ohm resistor, a KN-22 Krytron switch tube, and a 0.0075-inch spark gap. The 30 percent firing point was selected as a representative test instead of the 50 percent point,

because of the 5-kV maximum voltage limitation of the Krytron for the test parameters used. One-hundred twenty tests were conducted over a period of 6 days and were analyzed as through they were the results of four sets of 30 trials each or two sets of 60 trials. A sample size of ten was found to be too small to give reproducible results.

The second reproducibility test was conducted for the zero firing point with a 330-pF capacitor and a 1.2 megohm resistor. Twenty-five trials were carried out at each test level. The excellent reproducibility of both tests is very likely inherent in the use of the parallel-plate electrodes. This point is elaborated upon in the DISCUSSION section.

Energy Response Curve

It was of interest to determine whether the data for the spark energies required to initiate lead azide (RD 1333) would fit a normal probability distribution curve. When the data for the complete firing curve were plotted on probability paper (Figure 3), they yielded essentially a straight line. This indicated that the data could be considered, for all practical purposes, to be normally distributed. Each point on the graph is the result of 25 tests for the following conditions: 0.0075-inch gap, 2850 pF capacitance, and 100 kilohms resistance. This result provides some justification for using the 50 percent firing point in the studies described in this report to characterize the sensitivity of the explosive.

TABLE 1

Reproducibility Tests Results for the Electrostatic Sensitivity Apparatus

a. 120 tests conducted at the 30 percent firing point for lead azide (RD 1333) (charging voltage = 4000 volts; series resistance = 56 ohms; storage capacitance = 2850 pF)

Analyzed as Four Sets of 30 Trials Each

8/30*	10/30	9/30	9/30

* (8 fired out of 30)

Analyzed as Two Sets of 60 Trials Each

18/60	18/60

b. Two tests, two weeks apart, of the zero firing point of lead azide (RD 1333) at 1.2 megohms and 330 pF

First Test: 8700 ergs total stored energy

Second Test: 9500 ergs total stored energy

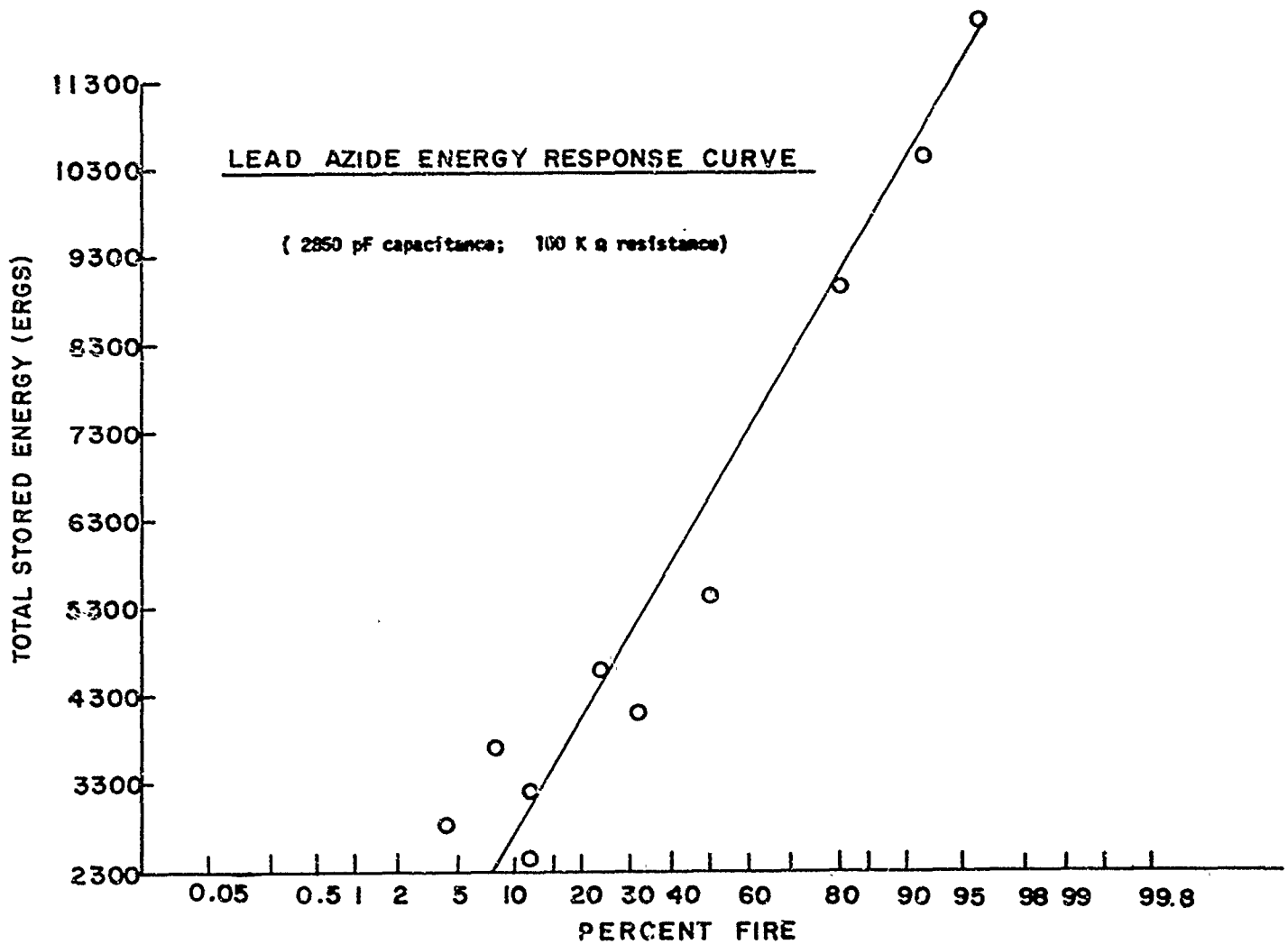
LEAD AZIDE ENERGY RESPONSE CURVE
(2850 pF capacitance; 100 K Ω resistance)
TOTAL STORED ENERGY (ERGS)
11300
10300
9300
8300
7300
6300
5300
4300
3300
2300
0.05
0.5
1
2
5
10
20
30
40
60
80
90
95
98
99
99.8
PERCENT FIRE

FIGURE 3

Energy in the Spark Gap

The energy dissipated in the spark gap was calculated for the different series resistance circuits from the current and voltage traces and is shown graphically in Figures 4 and 5 for the mercury and the Krytron switch circuits, respectively. The curves were drawn by visual inspection. The average is shown by the cross bar and standard deviation by the vertical distance. A dotted line was drawn in the smaller series resistance region (Figure 5) where the data were difficult to obtain, as discussed later. The technique for determining the energy dissipated in the spark gap is given in Appendix C.

The experimental data show that with a 0.005- to 0.0075-inch gap, the energy delivered to the spark gap decreased from approximately 80 percent of the total stored energy to 10 to 14 percent of the total as the series resistance was increased from 0.15 ohm to 1000 ohms. As the resistance was further increased to 1.2 megohms, the energy delivered remained practically constant at the 10 to 14 percent level. Very similar results have been obtained by Moore, Sumner and Wyatt[1]. They found that with a gap of 0.005 inch, a fairly constant value of about 10 percent of the original energy appeared in the spark gap when series resistances of 10^3 to 10^7 ohms were used. A possible explanation for this energy constancy is given in the Appendix of Reference 11.

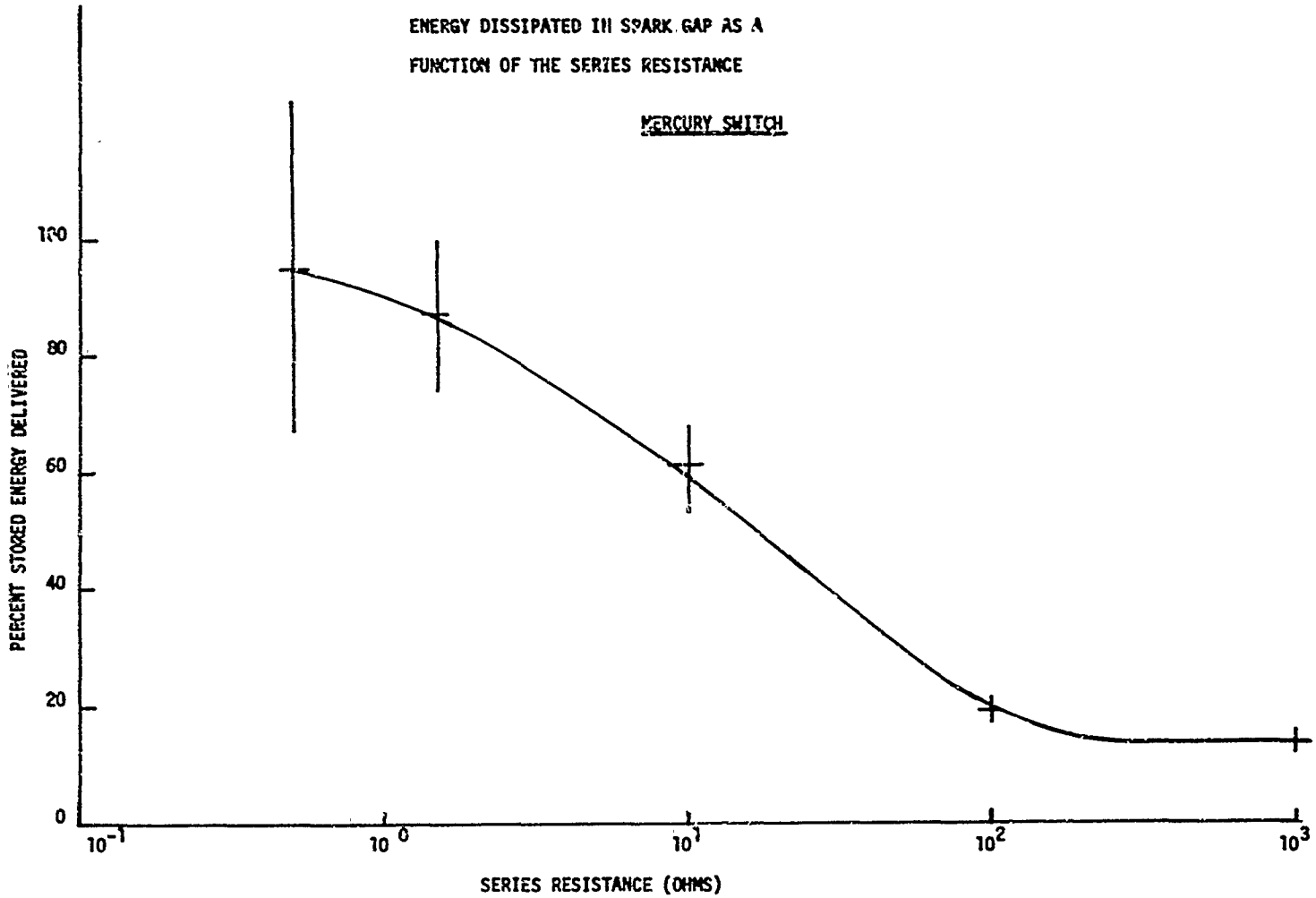
ENERGY DISSIPATED IN SPARK GAP AS A
FUNCTION OF THE SERIES RESISTANCE
MERCURY SWITCH
PERCENT STORED ENERGY DELIVERED
100
80
60
40
20
0
10^{-1}
10^{0}
10^{1}
10^{2}
10^{3}
SERIES RESISTANCE (OHMS)

FIGURE 4

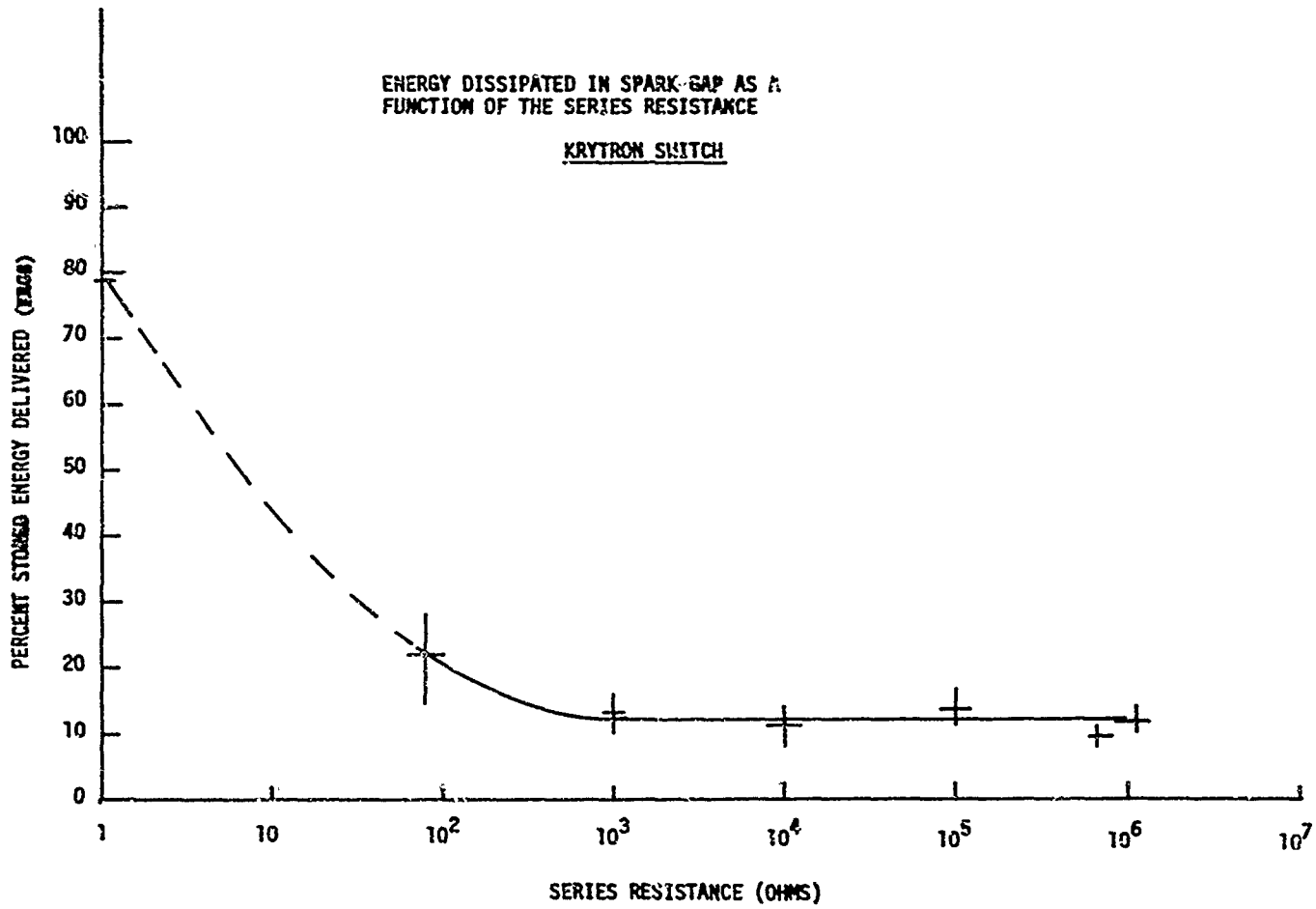
ENERGY DISSIPATED IN SPARK GAP AS A
FUNCTION OF THE SERIES RESISTANCE
KRYTRON SWITCH
PERCENT STORED ENERGY DELIVERED
100
90
80
70
60
50
40
30
20
10
0
1
10
10^2
10^3
10^4
10^5
10^6
10^7
SERIES RESISTANCE (OHMS)

FIGURE 5

The data for the small series resistance are of limited accuracy because of the difficulty of recording the fast current and voltage traces. With small series resistances in the circuit the durations of the sparks were in the hundreds of nanoseconds range. Because these times were too fast for the oscilloscope and photographic film being used current and voltage traces were very faint. Small errors in reading the peak current and voltage from the faint traces or a small time shift in aligning the start of the traces, of the order of 10 nanoseconds, could result in large errors in integrating the reduced current and voltage data.

The Effect of the Energy Delivery Rate on the Initiation of Lead Azide (RD 1333)

A. Series Resistance

It was shown that series resistance affects the total energy delivered to the spark (Figures 4 and 5). A systematic investigation was also carried out to determine what effect different series resistances have on the rate of energy delivery of a spark. This rate, in turn, would affect the initiation probability of lead azide (RD 1333). The RC time constant of the spark electrical circuit was increased from approximately 0.1 microsecond to 50 milliseconds by increasing in increments the series resistance from approximately 1 ohm to 15 megohms. A Krytron switch was used in all the experiments.

The energy level at the 50 percent firing point, determined by the "Bruceton" method[12], was used as a measure of sensitivity to minimize the number of tests required. As can readily be seen in Table 2 and in the graph of Figure 6, the energy required in the gap at the 50 percent points of initiation was a strong function of the series resistance in the discharge circuit. The energy decreased to a minimum as the RC time constant was increased from 0.1 microsecond to some value between 0.1 and 1 millisecond, and then increased as the RC time constant was further increased to 43 milliseconds.

An important observation should be noted. It took less energy in the gap to get 50 percent initiation in the 0.1 to 1 millisecond RC time constant range than at either extreme. This range, which is the most hazardous (the value for the series resistance and the storage capacitance which resulted in a minimum delivered energy), is treated further in the next section and in the DISCUSSION.

B. Storage Capacitance

The dependence of the initiation probability of lead azide (RD 1333) on the storage capacitance is shown in Table 3 and in the graph of Figure 7. As the capacity of the storage capacitors was decreased from 2850 pF to 330 pF (the lowest capacitance tested) for three series resistances (100 K, 680 K and 1.2 M ohms), the minimum energy dissipated in the spark gap decreased from 2700 ergs to 1100 ergs. It is of interest to consider the RC time constants of the circuits (see Figure 8). The time constants for all combinations of capacitance

TABLE 2

The Effect of Series Resistance on the Initiation of Lead Azide (RD 1333)

(50 Percent Firing Point; 2250-pF Capacitance; Parallel-Plate Electrodes)

Series Resistance (ohms)	RC Time Constant (milliseconds)	Spark Duration (microseconds)	Charging Voltage (volts)	Total Stored Energy, 1/2 CV^2 (ergs)	Energy in Spark Gap (ergs)
0.15	*	~0.1	2500	89,000	80,000
56	1.6×10^{-4}	0.7	>4000	>230,000	>50,000
1.0K	2.9×10^{-3}	10	>4000	>230,000	>28,000
5.1K	1.5×10^{-2}	45	2900	120,000	14,400
10K	2.9×10^{-2}	60	2250	72,000	8,600
100K	2.9×10^{-1}	350	1950	54,000	6,500
680K	1.9	1,200	2100	63,000	7,600
1.5M	4.3	---	2150	66,000	7,900
6.8M	19	---	2650	100,000	12,000
15M	43	22,000	2850	120,000	14,400

*Self-commutated by Krytron Switch

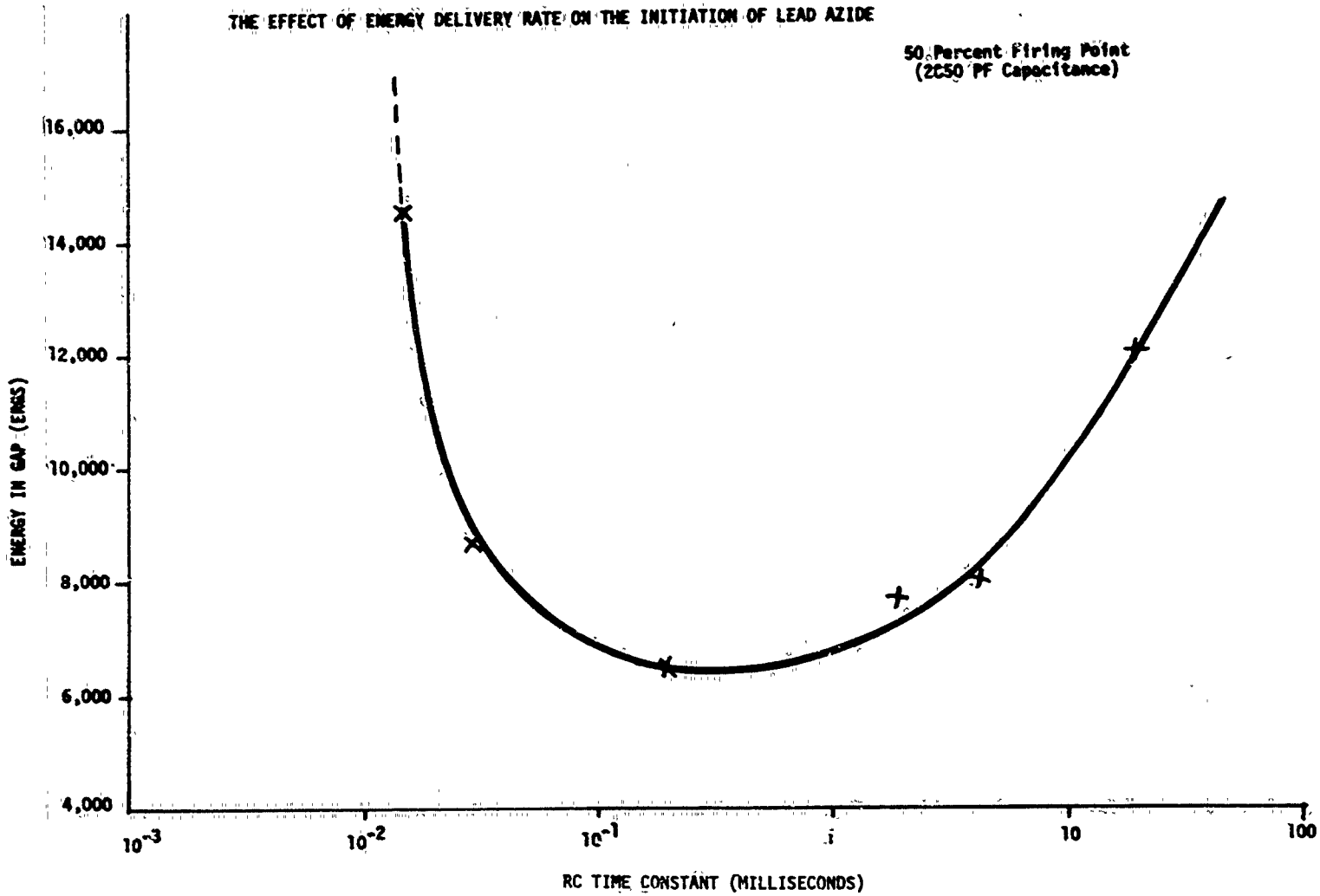
THE EFFECT OF ENERGY DELIVERY RATE ON THE INITIATION OF LEAD AZIDE
50 Percent Firing Point
(2C50 PF Capacitance)
ENERGY IN GAP (ERGS)
16,000
14,000
12,000
10,000
8,000
6,000
4,000
10^{-3}
10^{-2}
10^{-1}
1
10
100
RC TIME CONSTANT (MILLISECONDS)

FIGURE 6

TABLE 3

The Effect of Capacitance on the Initiation of Lead Azide RD 1333

(Minimum Energy; Parallel-Plate Electrodes)

	Capacitance (330 pF)				Capacitance (530 pF)			
Series Resistance (ohms)	RC Time Constant (milliseconds)	Charging Voltage (volts)	Total Stored Energy (ergs)	Energy in Spark Gap (ergs)	RC Time Constant (milliseconds)	Charging Voltage (volts)	Total Stored Energy (ergs)	Energy in Spark Gap (ergs)
100K	3.3×10^{-2}	4000	26,400	3,100	5.3×10^{-2}	2750	20,000	2,400
680K	2.2×10^{-1}	3000	14,900	1,800	3.6×10^{-1}	2400	15,300	1,800
1.2M	4.0×10^{-1}	2350	9,100	1,100	6.4×10^{-1}	2700	19,300	2,300

	Capacitance (990 pF)				Capacitance (1860 pF)			
Series Resistance (ohms)	RC Time Constant (milliseconds)	Charging Voltage (volts)	Total Stored Energy (ergs)	Energy in Spark Gap (ergs)	RC Time Constant (milliseconds)	Charging Voltage (volts)	Total Stored Energy (ergs)	Energy in Spark Gap (ergs)
100K	9.9×10^{-2}	1850	16,900	2,000	1.9×10^{-1}	1450	19,600	2,350
680K	6.7×10^{-1}	1850	16,900	2,000	1.3	1700	26,900	3,200
1.2M	1.2	2100	21,800	2,600	2.2	1450	19,600	2,350

TABLE 3 (Continued)

The Effect of Capacitance on the Initiation of Lead Azide (RD 1323)

(Minimum Energy; Parallel-Plate Electrodes)

Series Resistance (ohms)	Capacitance (2850 pF)			
	RC Time Constant (milliseconds)	Charging Voltage (volts)	Total Stored Energy (ergs)	Energy in Spark Gap (ergs)
100K	2.9×10^{-1}	1250	22,300	2,700
680K	1.9	1600	36,500	4,400
1.2M	3.4	1800	46,000	5,500

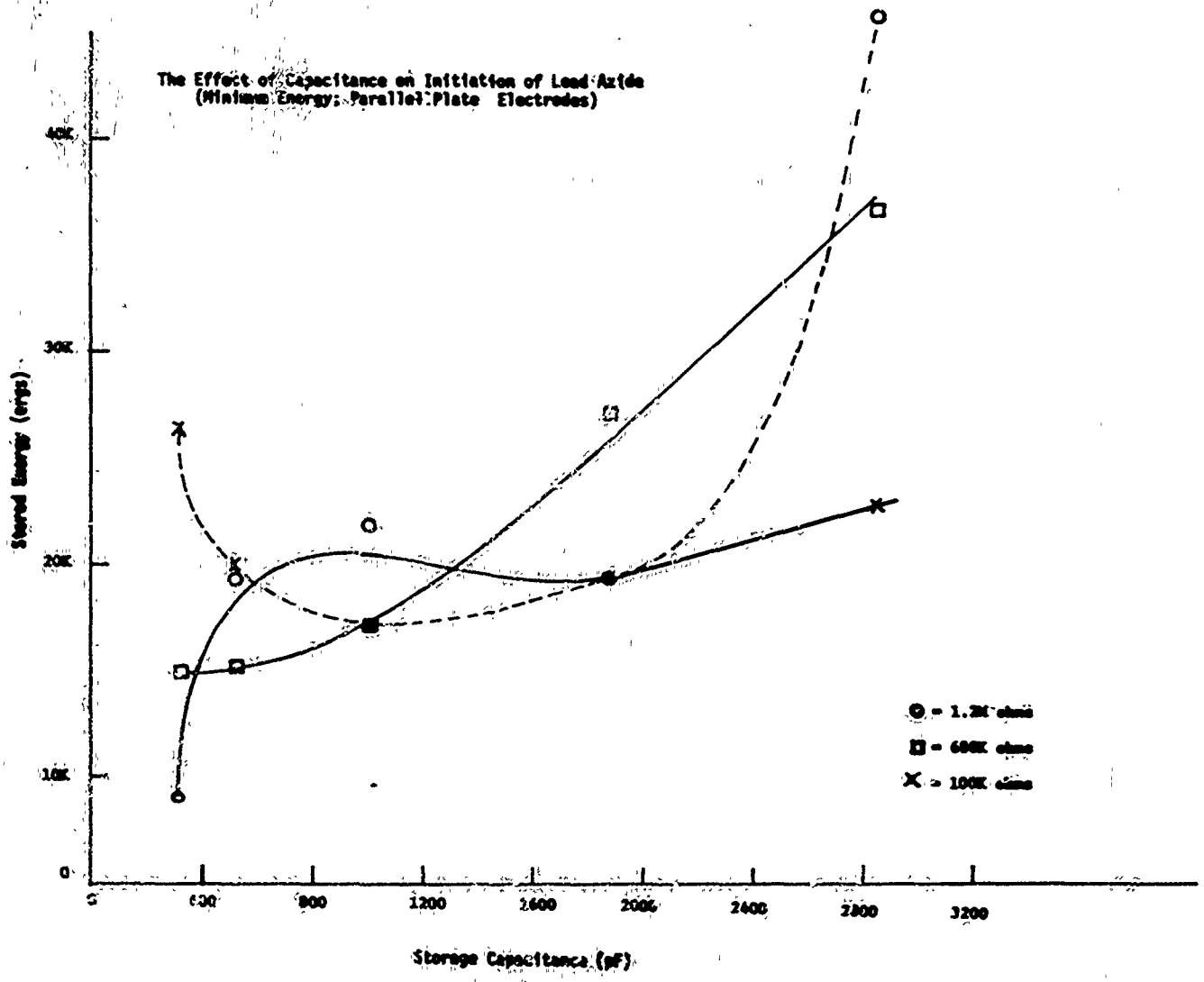
The Effect of Capacitance on Initiation of Lead Azide
(Minimum Energy; Parallel Plate Electrodes)
Stored Energy (ergs)
40K
30K
20K
10K
0
0
400
800
1200
1600
2000
2400
2800
3200
Storage Capacitance (pF)
= 1.2M ohms
= 680K ohms
= 100K ohms

FIGURE 7

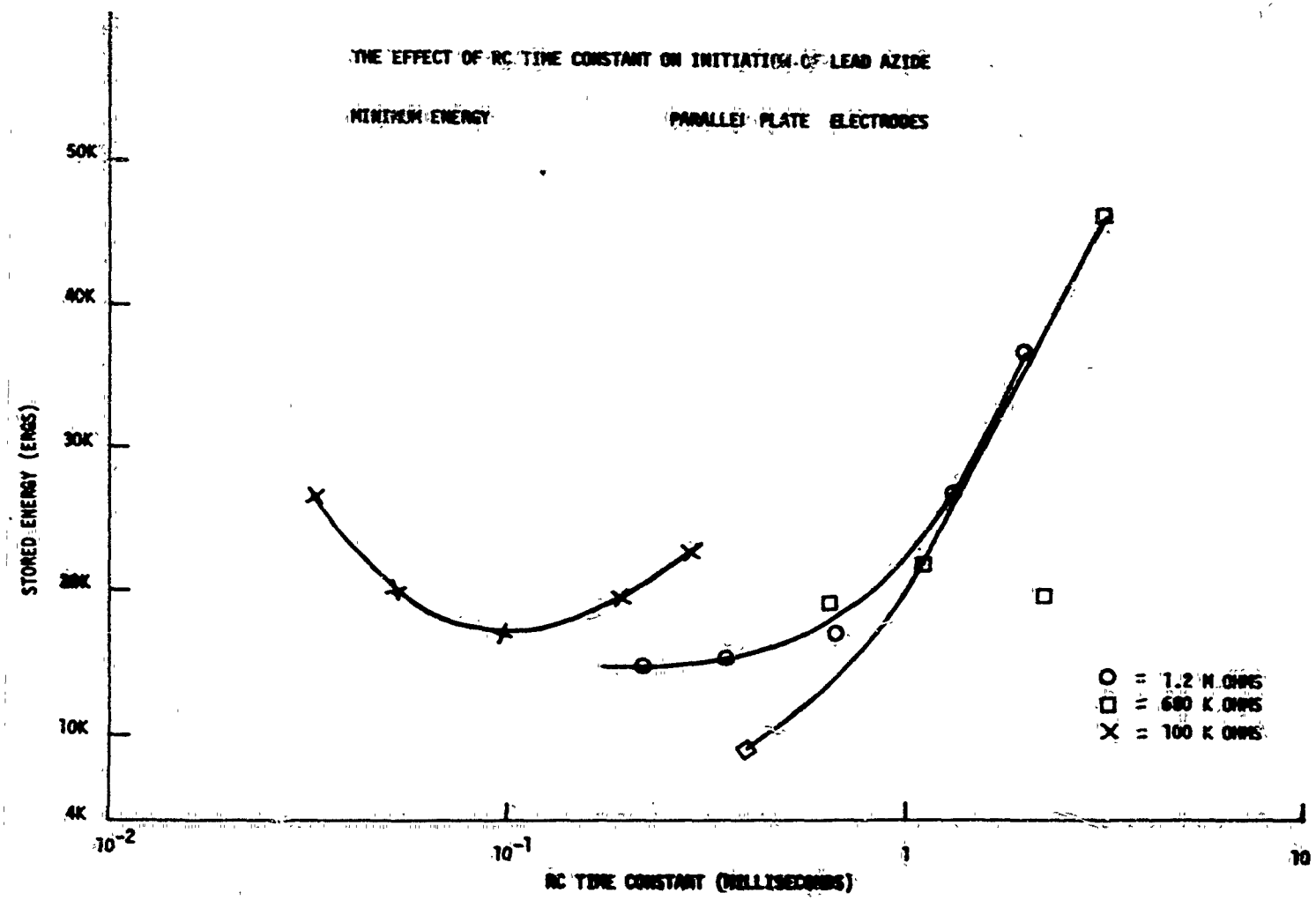
THE EFFECT OF RC TIME CONSTANT ON INITIATION OF LEAD AZIDE
MINIMUM ENERGY
PARALLEL PLATE ELECTRODES
STORED ENERGY (ERGS)
50K
40K
30K
20K
10K
4K
10^{-2}
10^{-1}
1
10
RC TIME CONSTANT (MILLISECONDS)
O = 1.2 M OHMS
□ = 680 K OHMS
X = 100 K OHMS

FIGURE 8

and resistance which resulted in a minimum initiation energy were approximately the same, 0.1 to 0.4 millisecond. This suggests that there is a most hazardous RC time constant which would result in the initiation of lead azide by the least amount of energy being dissipated in the spark gap.

It is noteworthy that the lowest initiation energy was observed with the smallest capacitance tested. This capacitance is in the range that is expected to be found in the normal handling and processing of primary explosives.

For the 2850- and the 1860-pF storage capacitors with a 100 kilohm series resistance the reported minimum energy values were actually the threshold for gap breakdown. For both these capacitances, the actual voltage developed across the spark gap was approximately 1200 volts. Gap breakdown did not occur as can be seen from the current and voltage traces (Figure 9). As the capacitance was decreased, higher voltages were required to initiate the explosive. The higher the applied voltage is above the spark threshold voltage, the larger the electrical current flow. The characteristics of a high current flow spark probably account for the lower initiation energies observed with the smallest capacitance.

The energy values at the 50 percent initiation points for lead azide were determined for three different storage capacitors (Table 4). These energy values decreased only slightly as the capacitance was decreased from 2850 to 1000 pF for a 100-kilohm series resistance.

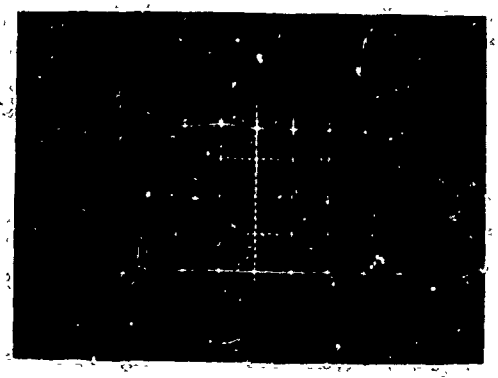

NO GAP BREAKDOWN

(Resistance: 100 kilohms; Capacitance: 2850 pF; Upper vertical trace: Voltage across spark gap and series resistance, 500 volts/division; Lower vertical trace: Voltage across series resistance, 500 volts/division; Time of traces: 50 microseconds/division)

FIGURE 9

TABLE 4

50 Percent Initiation Points

(100 kilohms Series Resistance)

Explosive	Capacitance (pF)	RC Time Constant (milliseconds)	Charging Voltage (volts)	Total Stored Energy (ergs)	Energy in Spark Gap (ergs)
	990	9.9×10^{-2}	3050	46,000	5,500
Lead Azide	1860	1.9×10^{-1}	2250	47,000	5,600
	2850	2.9×10^{-1}	1950	54,000	6,500
Lead Styphnate	990	9.9×10^{-2}	2100	22,000	2,600

To demonstrate that the apparatus can be used to distinguish between two primary explosives, the energy value at the 50 percent initiation point for basic lead styphnate (Lot No. OMC-68-14) was determined and was compared to that of lead azide (Table 4). As expected, there was a considerable difference in the energies. The energy required to initiate lead styphnate was less than one-half of that needed for lead azide for the particular test condition. It is apparent that the apparatus can distinguish the difference between the initiation threshold of lead azide and that of lead styphnate.

C. Needle-Plane Electrodes

The study carried out to compare the spark discharge characteristics of the parallel-plate electrodes with those of the more conventional needle-plane configuration showed that the threshold voltages for gap breakdown were much higher for the needle-plane configuration. For example, with a 0.0075-inch needle-plane gap, a spark was not observed for voltages as high as 4000 volts, whereas only 1250 volts were required for the parallel-plate configuration. When the needle gap was reduced to 0.0025 inch, the threshold voltage was still 1750 volts.

It is interesting to note, in addition, that when either an inert powder or lead azide was placed in the gap, a threshold voltage as low as 1300 volts was observed for a 0.010-inch needle-to-plane gap (needle buried in the powder). On the other hand, the addition of powder to the 0.0075-inch gap of the parallel-plate electrodes inhibited sparking and increased the threshold voltage required to break

down the gap. This phenomenon concerning the threshold voltages for gap breakdown is treated in the DISCUSSION.

Table 5 compares the minimum initiation energy values for lead azide (RD 1333) obtained by means of the needle-plane electrodes with those of the parallel-plate electrodes using a 330-pF capacitance and a range of series resistances. Values for the needle-plane electrodes were much higher than those for the parallel-plate configuration. It should be noted that the needle-plane electrode configuration, as for the parallel-plate electrodes, yielded lower initiation energies for RC time constants in the range of 0.1 to 1 millisecond.

DISCUSSION

Rate Effect

Experimental work has shown that the energy of initiation of lead azide (RD 1333) by gaseous discharge was a strong function of the electrode geometry and the properties of the discharge circuit. The series resistance and the storage capacitance affected the discharge rate governing energy delivery to the spark gap. The threshold initiation energy of lead azide was considerably decreased when the duration of the spark was increased from 100 nanoseconds to hundreds of microseconds by the introduction of a large series resistance. The least amount of energy delivered to the spark gap for initiation was observed when the RC time constant was in the 0.1 to 1 millisecond range.

TABLE 5

Comparison of the Minimum Initiation Energy of Lead Azide RD 1333 Obtained by the Needle-Plane Electrodes and the Parallel-Plate Electrodes

(330 pF Capacitance)

Series Resistance (ohms)	RC Time Constant (milliseconds)	Charging Voltage (volts)		Energy in Spark Gap (ergs)	
		Needle-Plane	Parallel-Plate	Needle-Plane	Parallel-Plate
0.15	*	3,000	1,500	13,000	3,300
82	2.7×10^{-5}	>4,000	2,900	> 5,900	3,100
100K	3.3×10^{-2}	>4,000	4,000	> 3,100	3,100
680K	2.2×10^{-1}	3,300	3,000	2,200	1,800
1.2M	4.0×10^{-1}	3,200	2,350	2,000	1,100

*Self-Commutated by Krytron Switch

Initiation Mechanism

The results show that energy delivery rate is an important parameter in the initiation of lead azide (RD 1333) and suggest a time-dependent process, presumably a thermal diffusion mechanism, in which a minimum spark (heat source) is maintained long enough to give rise to propagating self-supporting hot-spot in the lead azide crystal.

With no series resistance in the circuit, the spark was visibly brighter and more violent. The maximum current was in the 30- to 100-ampere range (the maximum current was only milliamperes with large resistance). More than twice the energy required for the large series resistance experiments was delivered to the spark gap in 100 nanoseconds. It is possible that for these fast energy delivery rates, initiation may not be due to any single mechanism but to a complex combination of several mechanisms. For example, in addition to a thermal mechanism, radiation absorption may play an important role because the lowest wavelength and highest light density are present in this fast region. Mechanical shock from a fast discharge may also be a factor.

Safety

In evaluating the data from a safety point of view, these two markedly different energy delivery rates are of concern in a hazard analysis. The least amount of energy needed to initiate lead azide (RD 1333) by gaseous discharge was observed when the energy was delivered over a relatively long time, several hundreds of microseconds.

Since the efficiency of energy transfer for these long times is quite low, about 10 to 14 percent, a hazardous situation would not exist unless there was 7 to 10 times this minimum energy stored somewhere in the system and a large resistance to control the discharge. On the other hand, although three times as much delivered energy was required with zero resistance as with the large series resistance for initiation, the total stored energy necessary to deliver this energy was lower with the zero resistance because of the greater efficiency of delivery, approximately 80 to 95 percent of the stored energy. At the 50 percent initiation point, however, both the total stored energy and the delivered energy were at a minimum with the large series resistances.

Moore, Sumner and Wyatt[2] also found that some primary explosives, such as lead azide and lead styphnate, were sensitive to both fast and slow discharges. In addition, they found that other primary explosives, such as mercury fulminate and tetrazene, were primarily sensitive to slow discharges. Morris[13] found that lead styphnate is more sensitive to fast discharges (no series resistance). From a safety point of view, therefore, both fast discharges (zero resistance) and slow discharges (large series resistances) must be considered hazardous and must be of major concern to the process engineer.

The standard electrostatic sensitivity tests are usually conducted under specific test conditions, at best, designed to simulate a particular hazard. In general, no attempts are made to investigate the effects of the rate of energy delivery on spark sensitivity. The results,

consequently, cannot be used to evaluate all of the different handling situations to which an explosive may be exposed. If a complete assessment of the electrostatic hazard of an unknown material is required, then a thorough research program is necessary.

In many practical hazardous situations, an exact knowledge of the sensitivity of a particular explosive is not necessary. It is sufficient to know the relative sensitivity of the explosive being dealt with and then take appropriate precautions[14]. (A sensitive explosive can be defined as one that can be initiated with energies in the order of 2×10^5 ergs.) The electrostatic sensitivity tests considered in this report provide a comparison among the sensitivities of explosives, i.e., a ranking of their sensitivities. The tests could also be used to evaluate potential additives which might be used to reduce the electrostatic hazard of primary explosives.

Gap Breakdown

The shape of the electrode plays an important role in gaseous discharges. Lower threshold voltages for gap breakdown were observed for gaseous discharge in the parallel-plate configuration than in the needle-plane electrodes for a constant gap distance. The addition of powder, either inert or lead azide, to the gap decreased the threshold voltage for the needle-plane electrodes but increased it for the parallel-plate electrodes. A possible explanation for this phenomenon is photon feedback. When a gas begins to break down, photons are emitted in all

directions. In the unconfined needle-plane configuration, the photons could spread out and escape, whereas in the parallel-plate configuration the protons are confined between the two flat and polished electrodes (the photons which strike the anode are reflected back to the cathode). The photons striking the cathode cause emission of secondary electrons, which give rise to the development of a complete discharge.

The addition of powder to the gap has two opposing effects. It enhances the electric field in the spaces between the particles because of the dielectric properties of the powder. However, it also interferes with the action of the photon field and the secondary electrons which affect the development of a discharge. Apparently, for the parallel-plate configuration and for lead azide, the interference with the photon emission outweighed the enhancement of the electric field. With the needle configuration a lower threshold voltage was observed because photon emission initially played an unimportant role; hence, the strength of the electric field was the prime factor in the breakdown of the gap.

It is also possible that higher breakdown voltages observed for the needle-plane configuration occurred because the steel needles developed thin oxides of relatively high dielectric strength on their surfaces in the presence of air. Pitts[15] noted that oxides on a needle can triple the breakdown voltage required for a particular air gap, while the oxide film had only a small effect on flat electrodes because they had enough surface area. None of the tests conducted to date can determine which of the two models is appropriate.

Electrode Geometry

Initiation energy values for lead azide may have been lower for the parallel-plate electrodes (or, equivalently, initiation probability at a given energy may have been greater) because that configuration confined the powder more than did the needle-point geometry. The spark resulted in a rapid movement of air which tended to blow the powder away from the electric discharge. The parallel-plate electrode configuration used in this work, however, tended to confine the powder and permitted more efficient "coupling" between the discharge and the powder.

Another possible contributing factor was that a larger volume of the explosive was sampled with the parallel-plate configuration than with the needle-plane geometry where only the explosive near the needle was sampled. When large series resistances were in the circuit, the discharge was not a continuous one, but rather a series of bursts of sparks. The sparks in this series did not all follow the same path. With the larger surfaces of the flat electrodes, a larger portion of the explosive powder was sampled. Figure 10 shows an undetonated sample of lead azide in the explosive holder, magnified 15 times, after being exposed to a burst of sparks (1.2 megohm series resistance). The black specks on the surface of the lead azide crystals are free lead due to decomposition from the discharge and show the large area that was sampled.

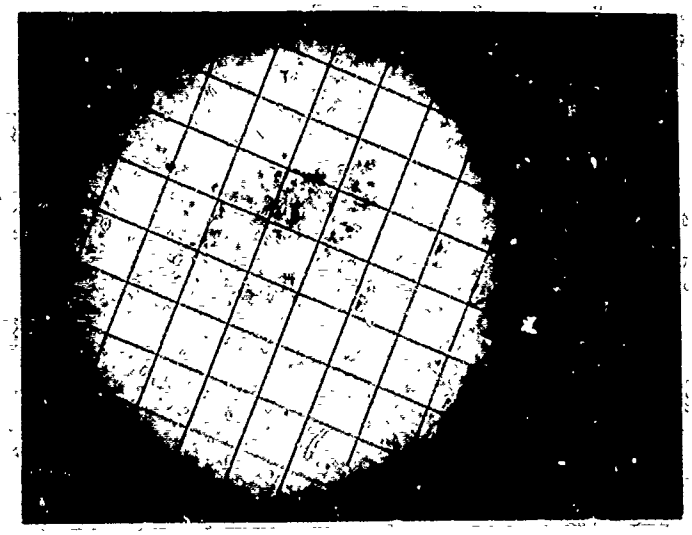

LEAD AZIDE POWDER AFTER SPARK DISCHARGE: NO DETONATION
(magnified 15 times)

FIGURE 10

CONCLUSIONS

1. There is a definite need for a versatile electrostatic sensitivity test apparatus and testing method that can be used for basic explosives research. The fixed spark-gap discharge apparatus with parallel-plate electrodes which was used in this study is versatile and is capable of yielding reproducible results.

2. The parallel-plate configuration yields a lower value for the minimum initiation energy of lead azide (PD 1333) than the needle-plane geometry. One of the problems with the needle-plane geometry is that the rapid movement of air resulting from the spark tends to blow the explosive powder away from the electric discharge. The parallel-plate electrode configuration tends to confine the powder and permits more efficient "coupling" between the discharge and powder. Another advantage of the parallel-plate configuration is that a larger volume of the explosive powder is sampled than with the needle-plane geometry where only the explosive powder near the needle is tested.

3. The addition of resistances in series with the spark gap changes the nature of the discharge and affects the fraction of the energy stored in the capacitor that is delivered to the spark gap. As the series resistance is increased, the form of the discharge changes from oscillatory (underdamped) to unidirectional (overdamped). With large series resistances (hundreds of kilohms), the discharge is no longer continuous but takes the form of a series of bursts of sparks due to

relaxation oscillations. As the series resistance is increased from zero to 1000 ohms, the energy fraction delivered to the 0.0075-inch spark gap decreases from 80 to 100 percent to 10 to 14 percent of the original stored energy. It then remains practically constant at this 10 to 14 percent level as the resistance is further increased to 1.2 megohm.

4. The sensitivity of lead azide (RD 1333) to gaseous discharge is not entirely dependent on the energy dissipated in the spark gap. Rather, it is a strong function of the electrode geometry and the properties of the discharge circuit, particularly the effects of the series resistances and the storage capacitors on the discharge rate. In all tests the lead azide (RD 1333) was initiated by gaseous discharge with the minimum energy when the RC time constant of the discharge circuit was relatively long, in the 0.1- to 1-millisecond range. This indicates that lead azide may be characterized by a "most hazardous RC time constant" which determines the optimum rate at which energy can be delivered to initiate the explosive. The results show that the energy delivery rate is an important parameter and suggest that a time-dependent process, possibly diffusion of heat from the spark channel into the azide crystal, is important for spark initiation.

5. From a safety point of view, both fast and slow spark discharges must be considered hazardous and must be of major concern to the process engineer. Some primary explosives are sensitive to both fast and slow discharges, while other primary explosives are sensitive to either one or the other.

6. The minimum delivered energy to initiate lead azide by gaseous discharge decreases as the capacitance is decreased to 330 pF (the smallest capacitance tested). For the smaller capacitances, larger currents flow in the spark discharge for a given delivered energy, indicating that the standard test procedure should use smaller capacitors. When large storage capacitors are used (1860 pF and above), electrostatic sensitivity apparatus may actually be determining the threshold voltage for gap breakdown rather than the minimum initiation energy for sensitive primary explosives.

7. The parallel-plate spark gap apparatus could easily distinguish between two primary explosives. For example, for a specific test condition, the energy value at the 50 percent initiation point for basic lead styphnate is less than one half of the value for lead azide (RD 1333) (see Table 4).

FUTURE WORK

1. The study will be extended to other primary explosives to determine their electrostatic sensitivities and whether these sensitivities can be characterized in terms of rate effects. The effects of temperature, humidity, gap length, and explosive particle size on the sensitivities of the explosives will also be investigated. These results will lead directly to the parameters needed for developing better standard test procedures. In order to determine these parameters, the following improvements and modifications will have to be made to the test apparatus:

a. Design and fabrication of a more efficient data reduction apparatus, possibly including an analog multiplier.

b. Design and evaluation of an inexpensive, mass-produced spark ampoule in which the electrodes are an integral part of the sample assembly. This ampoule will also allow the easy preparation of samples at a controlled humidity and temperature which then can be tested in an ordinary laboratory environment.

2. Future experimental work of a more fundamental nature could include the study of the nature of the spark and the determination of the characteristics of the spark gap in more detail in order to lead to a better understanding of electrostatic sensitivity. This program should include the following:

a. an attempt to characterize the spark discharge through its current voltage characteristics and to determine how the energy transfer efficiency depends upon applied voltage, capacitance and series resistance. Measurements to date seem to indicate that the efficiency is relatively independent of these variables over a wide range. However, this result is difficult to understand if one tries to analyze energy delivery using reasonable models for the spark characteristics. Also the current-voltage characteristics for small capacitances (330 pF) are very different from those for larger capacitances (2850 pF);

b. the determination of the current-voltage characteristics for different gaps, and gaps with explosives;

c. an attempt to study the size of the spark and the light output using photographic techniques;

d. an attempt to measure time-to-explosion using photo-optical or photometric techniques;

e. an attempt to determine the energy delivered to the spark gap at the fast delivery rates by integrating the voltage-charge phase portrait of the spark gap obtained by recording the charge transferred to a capacitor in series with the gap.

ACKNOWLEDGEMENTS

The author wishes to thank Professors C. R. Westgate (Johns Hopkins University) and L. Rosenthal (Rutgers University) for their helpful advice, Dr. B. Pollock for his helpful discussions, Mr. J. Hershkowitz for his constructive comments on the draft of the report, and Messrs. M. R. Buchanan and T. A. Graziano for their help in fabricating the test apparatus.

REFERENCES

1. P. W. J. Moore, J. F. Sumner, and R. M. H. Wyatt, "The Electrostatic Spark Sensitiveness of Initiators: Part I - Introduction and Study of Spark Characteristics." Explosives Research and Development Establishment Report 4/T/56, Waltham Abbey, Essex, England, 10 January 1956

2. P. W. J. Moore, J. F. Sumner, and R. M. H. Wyatt, "The Electrostatic Spark Sensitiveness of Initiators: Part II - Ignition by Contact and Gaseous Electrical Discharges." Explosives Research and Development Establishment Report 5/R/56, Waltham Abbey, Essex, England, 7 March 1956

3. P. W. J. Moore, "The Electrostatic Spark Sensitiveness of Initiators: Part III - Modification of the Test to Measure the Electrostatic Hazard Under Normal Handling Conditions." Explosives Research and Development Establishment Report 22/R/56, Waltham Abbey, Essex, England, 25 May 1956

4. D. B. Sciafe, "The Electrostatic Spark Sensitiveness of Initiators: Part IV - Initiation of Explosion by Spark Radiation." Explosives Research and Development Establishment Report 9/R/59, Waltham Abbey, Essex, England, 13 August 1959

5. R. M. H. Wyatt, "The Electrostatic Spark Sensitiveness of Initiators: Part V - Further Study of Ignition with Metallic and Antistatic Rubber Electrodes." Explosives Research and Development Establishment Report 24/R/59, Waltham Abbey, Essex, England, 4 September 1959

6. R. M. H. Wyatt, P. W. J. Moore, R. J. Adams, and J. F. Sumner, "The Ignition of Primary Explosives by Electric Discharges," Series A - Mathematical and Physical Sciences, Proceedings of the Royal Society, Vol 246, No. 1245, 29 July 1958

7. R. M. H. Wyatt, "The Electrostatic Spark Sensitivity of Bulk Explosives and Metal/Oxidant Mixtures," NAVORD Report 6632, June 1959

8. M. S. Kirshenbaum and R. R. Fyfe, "Electrification in Flow of Alcohol-Freon Mixtures Through Solid Filter Beds," Picatinny Arsenal Technical Report 4193, June 1971

9. B. D. Pollock, W. B. Zimny and C. R. Westgate, "Electrification of Lead Azide Powders Under Ambient Conditions," Picatinny Arsenal Technical Report 4214, June 1971

REFERENCES (Continued)

10. C. R. Westgate, B. D. Pollock, and M. S. Kirshenbaum, "Electrostatic Sensitivity Testing for Explosives," Picatinny Arsenal Technical Report 4319, April 1972

11. R. F. Gentner, "An Electrostatic Spark Sensitivity Test of Composition B," Picatinny Arsenal Technical Report 4119, December 1970

12. M. G. Natrella, "Engineering Design Handbook, Experimental Statistics, Section 2", Army Materiel Command Pamphlet 706-111, April 1965

13. G. Morris, "Ignition of Explosives by Condenser Discharges - Effect of Added Circuit Resistance," British Journal of Applied Physics, Supplement No. 2, March 1953, pS97-S100

14. "Explosive Hazard Assessment Manual of Tests: Test No. 6/66, The Electric Spark Test," Sensitiveness Collaboration Committee Explosives Research and Development Establishment. Procurement Executive Ministry of Defence, Waltham Abbey, Essex, England 1966.

15. L. D. Pitts, "Demythologizing Electrostatics," Franklin Institute, Proceedings of the Sixth Symposium on Electro-Explosive Devices, July 1969.

APPENDIX A

Description of Apparatus

The electrostatic sensitivity apparatus consisted of a charging circuit, a triggering circuit, the electrode assembly and a high speed dual beam oscilloscope.

Charging Circuit

High voltage was provided by a Precise Measurement Corporation variable 0-5 kilovolts power supply. The voltage was measured with a Model ESD Sensitive Research Electrostatic Voltmeter, either 0-2000 volts or 1500-5000 volts. Low inductance transmitting ceramic capacitors from Centralab (850 series) were used as the energy storage discharge capacitors. The circuit was designed so that the appropriate capacitance, from 25 to 10,000 pF, could be manually connected as either a single capacitor or a group of capacitors in parallel in the circuit. The capacitance of the storage capacitors and the stray capacitance of the electrical leads in parallel with the storage capacitor were measured in situ in the circuit using a General Radio Company Type 1656 Impedance Bridge.

Triggering Circuit

Fast, low-loss switches were used in the triggering circuit. For voltages up to 1000 volts, a JM1-120-11 mercury wetted contact relay, capable of nanosecond switching speeds, was used to transfer the potential of the selected capacitor to the spark gap. A schematic of the electronic circuit is shown in Figure 11.

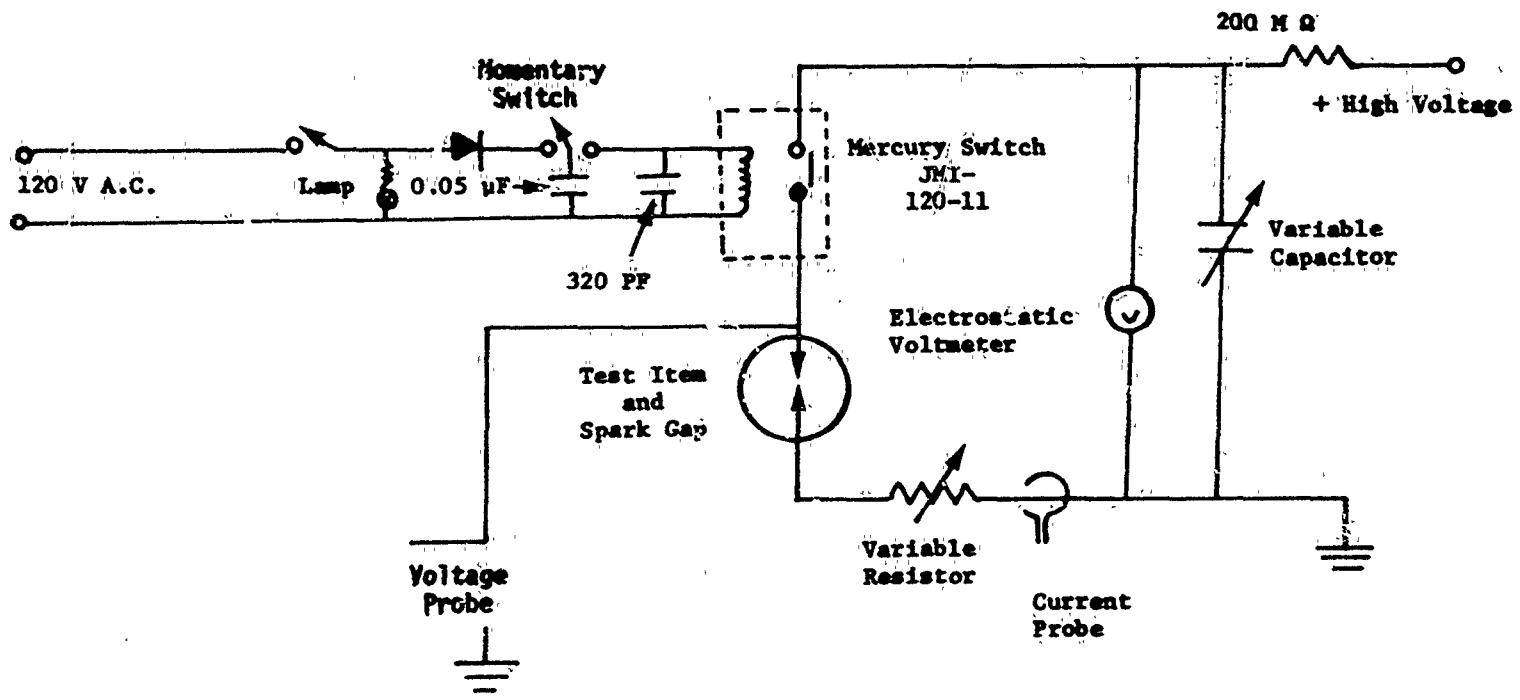

LOW VOLTAGE CIRCUIT

FIGURE 11

For higher voltages, a KN-22 Krytron (EG&G Inc) switch tube was used (Figure 12). The Krytron is a four-element cold-cathode gas filled fwitch tube which operates in an arc discharge mode in the 500-5000 volt range. The Krytron was triggered by an EG&G TR-130 trigger transformer.

The Electrode Assembly

The parallel-plate electrode assembly consisting of two 3/4-inch diameter steel plates is shown in Figures 13a and b. The spark gap containing the explosive is between the two electrodes. The lower portion of the upper electrode could be easily removed for cleaning purposes. It was slipped onto the shaft of the upper electrode assembly and was secured by a set screw. The base or lower electrode was connected to ground through a series resistor, which could be manually changed during testing. The upper portion of the base electrode served as the explosive sample holder. It was a detachable, solid cylinder of hardened steel, 3/4-inch diameter x 3/8-inch long. A layer of 0.0075-inch thick electrical tape with a 3/16-inch diameter hole for the explosive was taped to the top surface of the steel cylinder. The explosive powder in the hole was semiconfined between the upper electrode and the sample holder. The desired gap between the upper electrode and the sample holder was set and maintained by a fine screw adjustment knob which was connected to, but insulated from, the upper electrode and was located outside the firing chamber. The gap setting was read on a dial indicator attached to the fine screw adjustment knob.

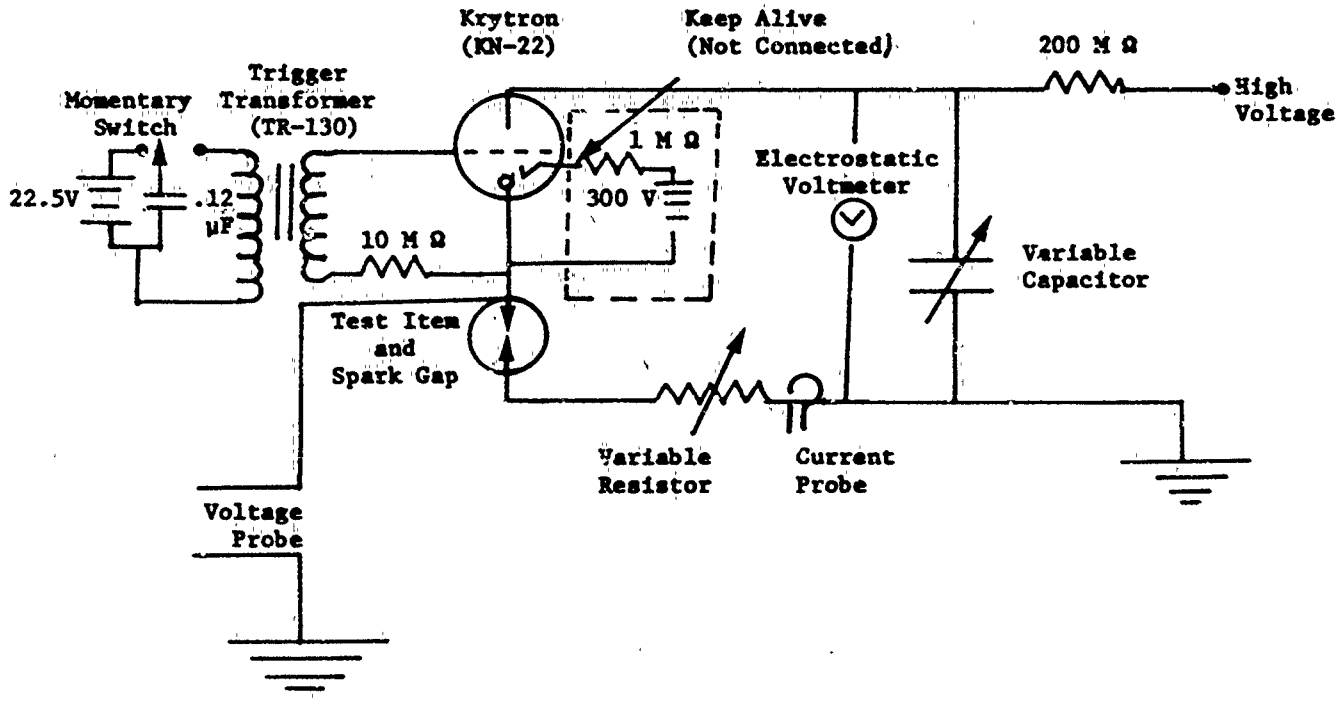

HIGH VOLTAGE CIRCUT

FIGURE 12

FIGURE 13a PARALLEL-PLATE ELECTRODE ASSEMBLY

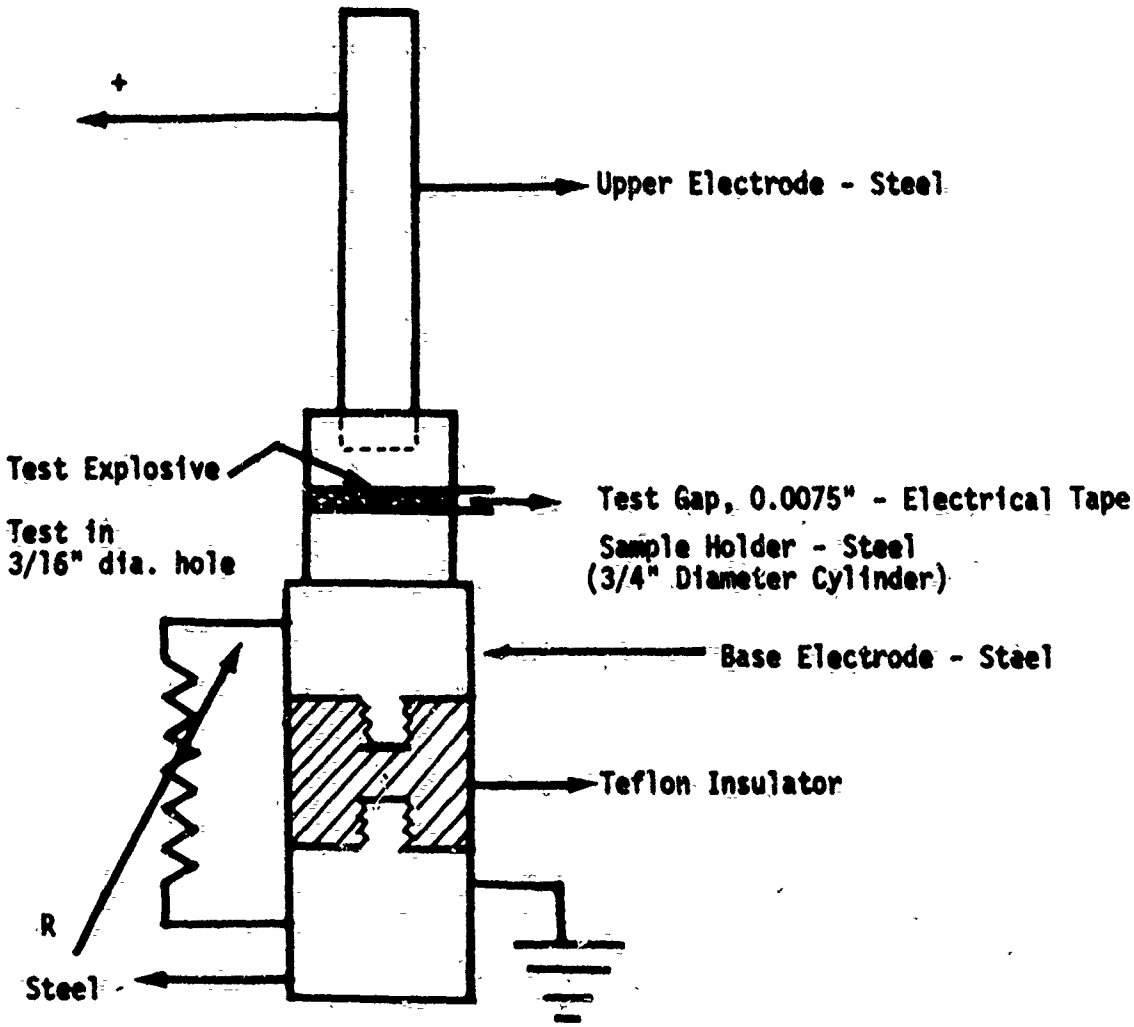

FIGURE 13b PARALLEL-PLATE ELECTRODE ASSEMBLY

The electrode assembly also could be used in the more conventional point-to-plane configuration. This was accomplished by substituting a phonograph needle holder (see Figure 14) with a removable phonograph needle for the upper electrode shaft.

The firing chamber (10-inch x 10-inch x 10-inch) was made of 1/2-inch thick clear plastic (Lucite ®) and sized to fit into a available humidity control box for future humidity controlled experiments.

High Speed Oscilloscope

The current and voltage characteristics of the spark were recorded photographically on a dual beam Tektronix 555 oscilloscope using a P6013A high voltage probe with a Type L Plug-In and a CT-2/P6041 current probe with a Type K Plug-In. The oscilloscope has a time base from 100 nanoseconds to 5 seconds per centimeter. The voltage probe has a built-in 1000:1 attenuation circuit and a rise time of 14 nanoseconds. The current probe can register currents from 10 milliamperes to 100 amperes. When a large resistor was used in series with the spark gap, the current was too low to give a deflection on the oscilloscope and, consequently, the current probe could not be used. Instead, a second P6013A voltage probe with a Type K Plug-In was used to measure the voltage drop across the series resistor to determine the current. The instantaneous current was taken as V_R/R where, V_R was the instantaneous potential drop across the resistor, R.

Carbon resistors with wattage ratings ranging from 1/4 to 1 watt were used for the series resistors. The values of the resistances for high current and voltage pulses were measured and were found to be the same as the low voltage, direct current resistances.

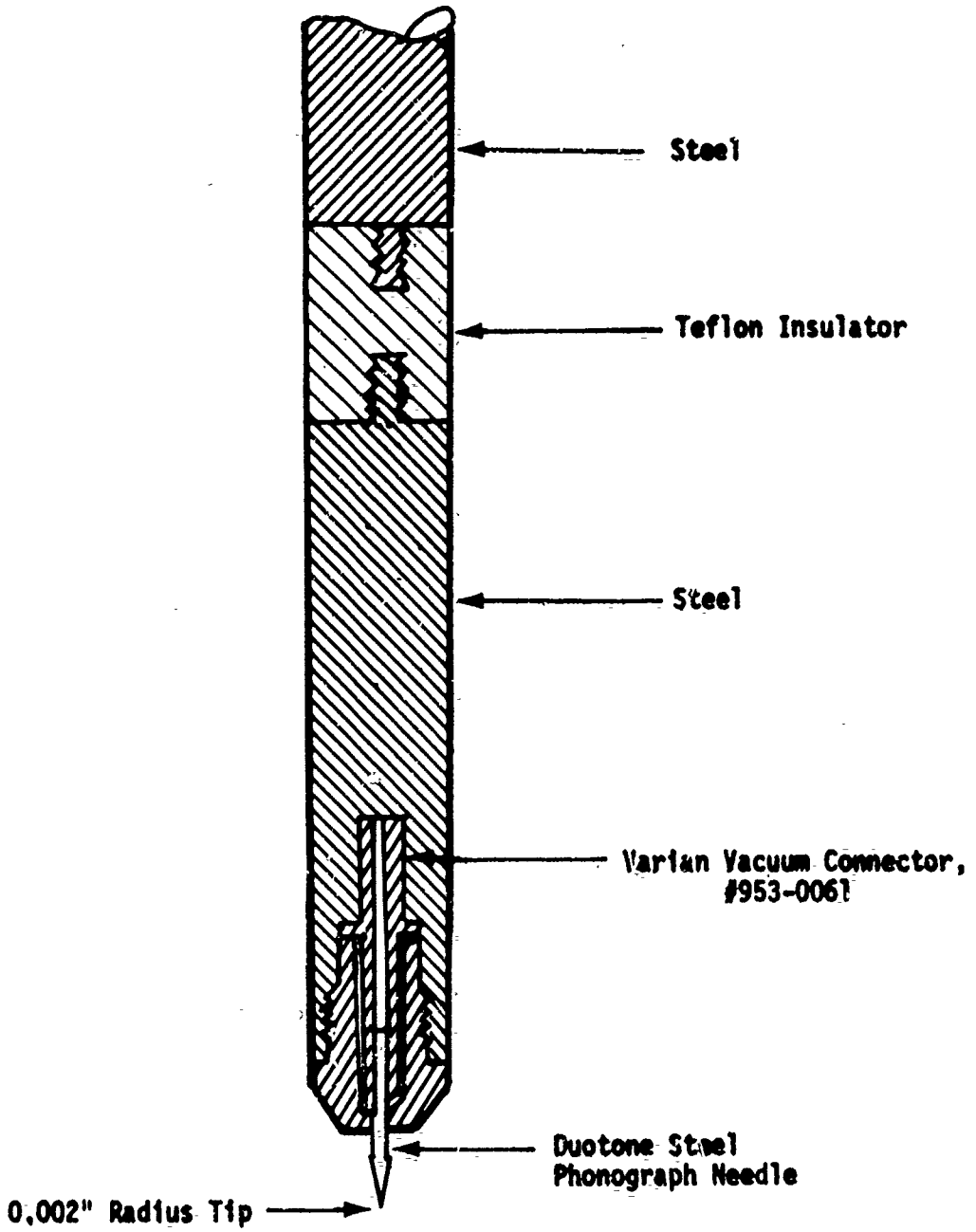

FIGURE 14 NEEDLE ASSEMBLY

APPENDIX B

Spark Discharge Characteristics

A study was carried out to characterize the spark discharge in air for the experimental testing apparatus as a function of the capacitance and resistance in the spark discharge circuit. This study showed that, when a mercury switch was used to transfer the voltage from the charged capacitor to the spark gap, the presence of the spark gap did not substantially alter the conventional capacitor discharge pattern. The spark gap only introduced a source of variable resistance. A detailed discussion of the conventional theory may be found in Reference 1.

Following conventional theory, it was found that the addition of circuit resistances from a few ohms to 15 megohms had a twofold effect. First, it primarily affected the form of discharge. It changed the oscillatory (underdamped) current and voltage to unidirectional (overdamped) waveforms (Figures 15a through 15f). Figure 15a shows the waveforms of the current through the spark gap and the voltage across the spark gap and series resistance when a 1800-pF capacitor charged to 900 volts was discharged to ground through the spark discharge circuit containing a 0.005-inch spark gap with no added circuit resistance. As can be seen, the current and voltage varied with time in an oscillatory manner because of the inherent inductance of the circuit. The voltage and current were slightly out of phase, the voltage leading the current.

500 V/div

20 A/div

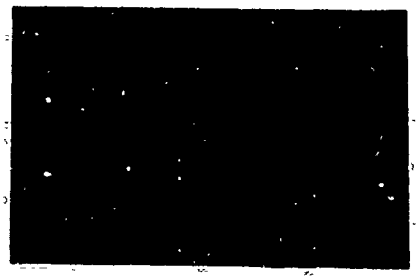

100 nsec/div

(a) R = 0.15 ohm

500 V/div

20 A/div

100 nsec/div

(b) R = 0.78 ohm

500 V/div

20 A/div

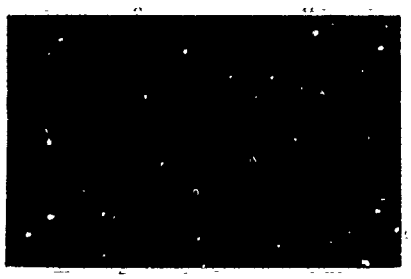

100 nsec/div

(c) R = 1.9 ohms

FIGURE 15

500 V/div

20 A/div

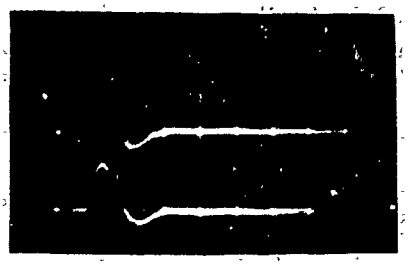

100 nsec/div

(d) R = 10 ohms

500 V/div

2 A/div

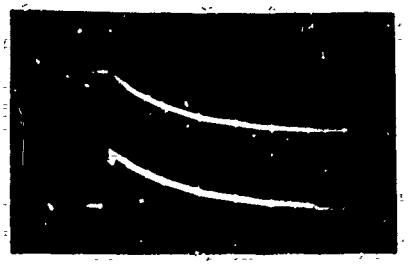

200 nsec/div

(e) R = 200 ohms

200 V/div

0.5 A/div

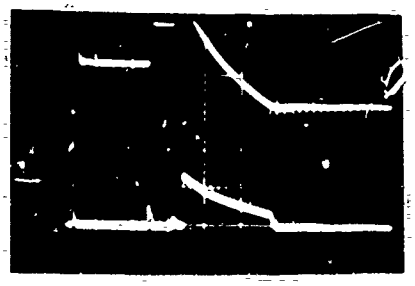

1000 nsec/div

(f) R = 1000 ohms

FIGURE 15 (Continued)

From the oscillograms, it can also be seen that the introduction of a 1.9-ohm resistor to the circuit reduced the number of oscillations from 4 to 2, and a 10-ohm resistor reduced the number to one. The current and voltage became critically damped (barely unidirectional) with about 15 to 20 ohms. With 200 ohms (Figure 15e) the discharge was unidirectional (overdamped).

The stray inductance responsible for the oscillatory discharge can be estimated from the decay of the current trace as a function of time by means of the following formula:

$$L = \frac{(t_2 - t_1)^2}{C\,[4\pi^2 + (\ln \frac{I_1}{I_2})^2]}$$

where L is the inductance in henries, C is the capacitance in farads, and t_1 and t_2 are the times in seconds for the values of two consecutive peak currents, I_1 and I_2. Calculations based on the above formula show that the stray inductance of the experimental apparatus was approximately 0.55 microhenry.

In addition to changing the oscillatory character of the discharge, the effect of increasing the series resistance was to change the duration of the spark and thus change the energy delivery rate. The effective spark duration time, estimated from the photographs, decreased from ap proximately 800 nanoseconds for no added resistance to a minimum value of approximately 100 nanoseconds for 15 ohms. One then

observed the conventional lengthening of the discharge time with further increases of resistance (see Table 6 and Figure 15). Note the changes in time scale in Figure 15.

The second effect was to reduce the fraction of the energy stored in the capacitor that was delivered to the spark gap. This effect is considered in detail in the RESULTS section of the report (Energy in the Spark Gap).

The effect of increasing the capacitance in the circuit can be seen by comparing Figures 15 and 16. It is also shown in Table 6. An increase in the capacitance increased the duration of the discharge in addition to increasing the energy available to the spark.

When a KN-22 Krytron switch tube was used in place of the mercury switch to transfer the voltage from the capacitor to the spark gap, oscillatory discharges were not as easily obtained as with the mercury switch since the Krytron provides some rectification of the current. With series resistances above about 20 ohms, however, similar but longer duration waveforms were obtained. Figures 17a through d show the typical current and voltage waveforms when a 1800-pF capacitor charged to 1900 volts was discharged to ground through the spark gap with different resistances in the spark gap circuit. In Table 6 typical spark durations for different resistances are compared with those obtained with the mercury switch.

TABLE 6

Dependence of Spark Duration on Series Resistance and Capacitance

(Parallel-Plate Electrodes)

Series Resistance (ohms)	Spark Duration (microseconds)					
	Mercury Switch			Krytron Switch		
	C=500pF	C=1800pF	C=3500pF	C=500pF	C=1000pF	C=1800pF
0.15	0.3	0.8	0.8	*	*	*
2.5	0.25	0.4	0.5	0.1	0.1	0.15
10	0.12	0.2	0.4	0.08	0.09	0.1
15	—	0.1	—	—	—	—
56	—	—	—	0.1	0.3	0.5
200	0.3	0.6	0.8	0.5	1.0	1.0
1000	0.8	2.5	4.0	1.5	2.5	3.6
5000	3.5	10	—	5	15	22

*Self-commutated by Krytron Switch

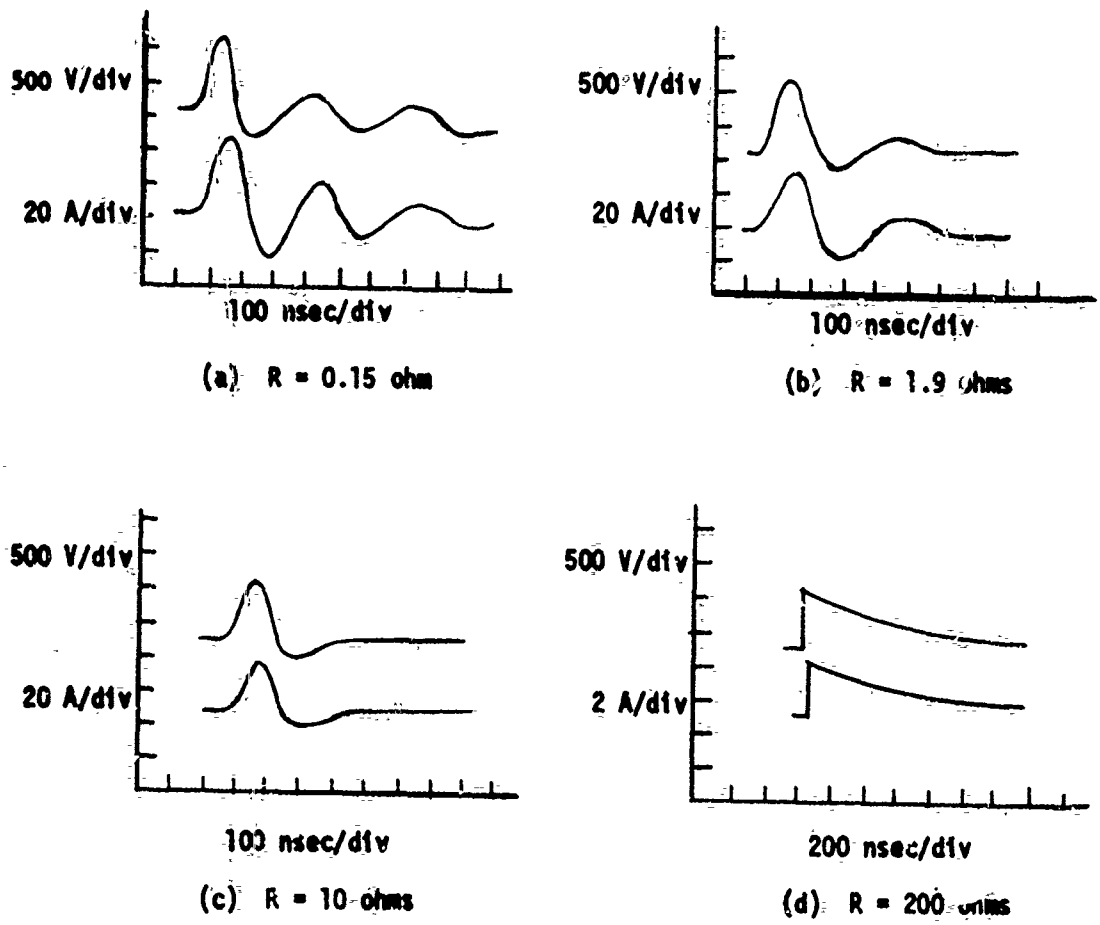

FIGURE 16 Typical Current and Voltage Characteristics of a Spark with Mercury Switch: 3500-pF Capacitance

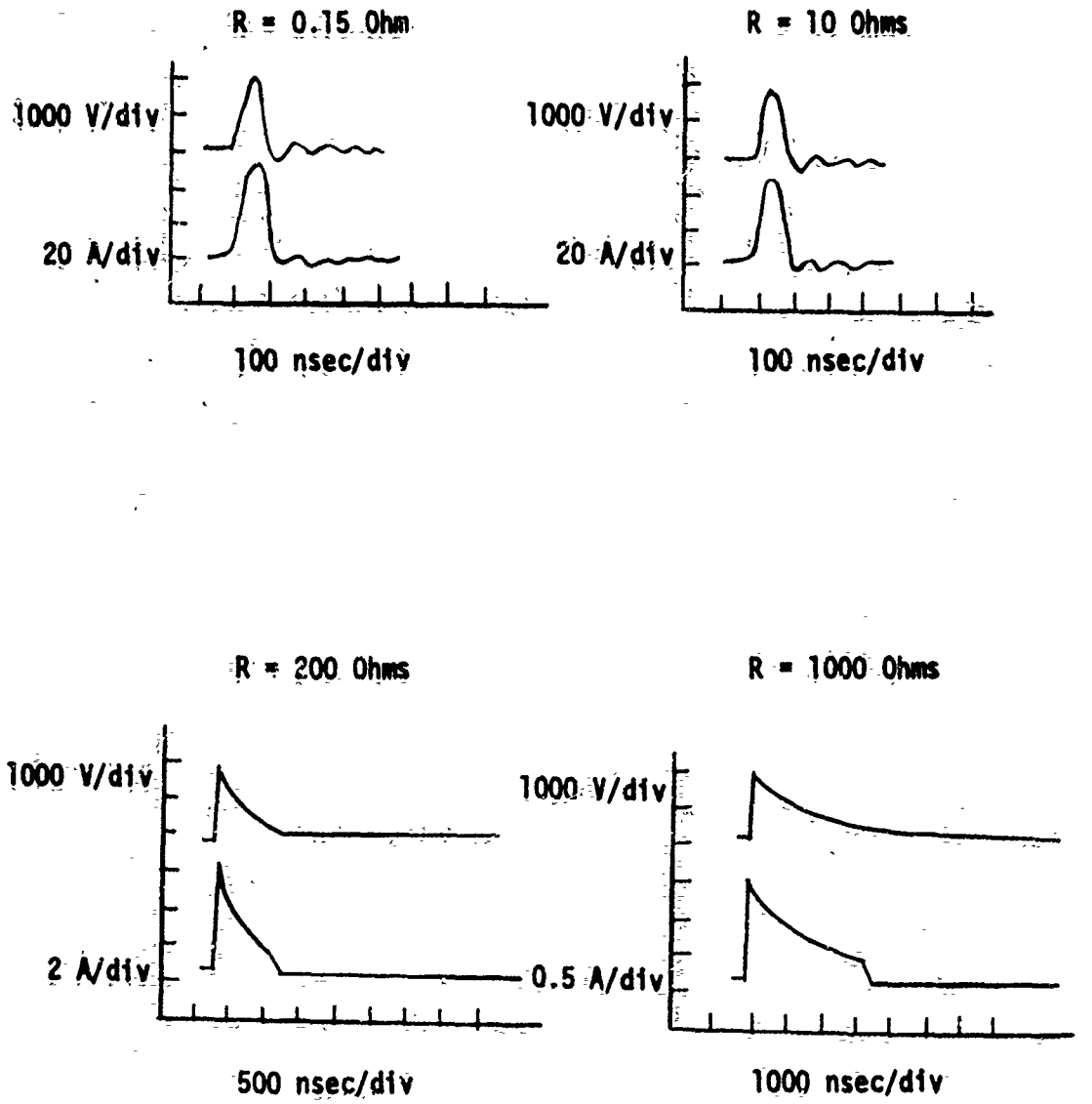

FIGURE 17 Typical Current and Voltage Characteristics of a Spark (Krytron Switch; 1800-pF Capacitance)

It was also noted that the discharge was not continuous but took the form of a series of burst of sparks when large series resistances were in the circuit. Typical current and voltage oscillograms for series resistances of 100 kilohms, 680 kilohms, and 1.2 megohms are shown in Figures 18a, b, and c, respectively. This phenomenon was due to relaxation oscillations. The relaxation oscillations were the result of the negative resistance of the spark gap and the stray capacitance of the electrodes. This explanation was verified by placing a 120-pF capacitor across the spark gap and observing that the frequency of the oscillations decreased (see Figures 19a and b).

When either an inert powder or lead azide RD 1333 was placed in the gap between the spark gap electrodes, little change was found in the current and voltage oscillograms. However, slightly higher threshold voltages were required to break down the gap and to cause a spark to pass than in air.

500 V/div

500 V/div

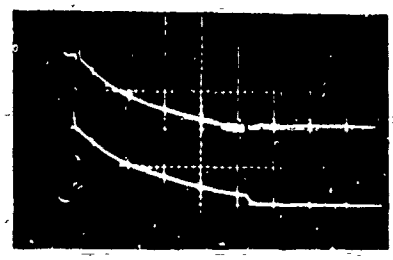

50 μsec/div

(a) R = 100 kilohms

500 V/div

500 V/div

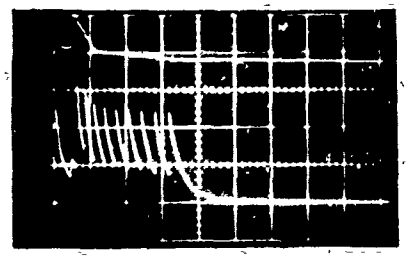

50 μsec/div

(b) R = 680 kilohms

1000 V/div

500 V/div

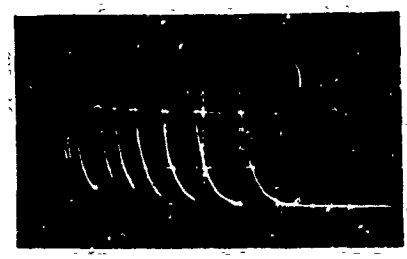

100 μsec/div

(c) R = 1.2 megohms

FIGURE 18 Typical Oscilloscope Traces of Voltage Across Spark Gap and Series Resistance During Spark Discharge with Krytron Switch: 1000-pF Capacitance (Upper vertical trace: Voltage across spark gap and series resistance; Lower vertical trace: Voltage across series resistance.)

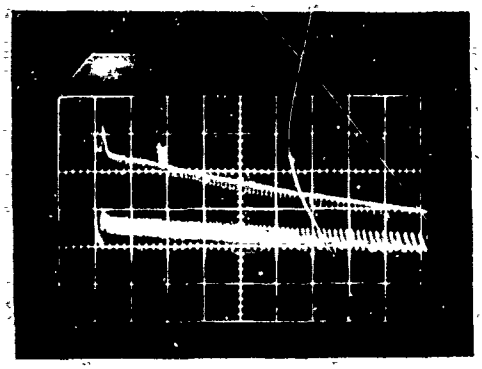

(a) Stray capacitance across the spark gap

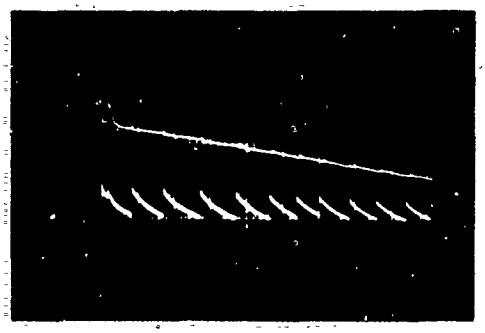

(b) 120-pF capacitor across the spark gap

FIGURE 19 Relaxation Oscillation Discharge. (Series resistance: 680 kilohms; Capacitance: 2200 pF; Upper trace: Voltage across spark gap and series resistance, 500 volts/division; Lower trace: Voltage across series resistance, 2000 volts/division; Time: 100 microseconds/division)

APPENDIX C

Energy Determination

The energy delivery rate, the energy actually delivered to the spark gap, and the fraction of the energy delivered as a function of time were determined from the photographs of the spark voltage and current traces. The energy delivered was determined by graphically integrating the current and voltage waveforms. This integration was accomplished by dividing the current and voltage curves into very samll time segments of duration δt and calculating the energy in the gap

$$\Sigma_{i=1}^{n} \left[\frac{(V_T I - I^2 R)_{i+1} + (V_T I - I^2 R)_i}{2}\right]\left[(t_{i+1} - t_i)\right]$$

and the energy in the resistance

$$\Sigma_{i=1}^{n} \left[\frac{(I^2 R)_{i+1} + (I^2 R)_i}{2}\right]\left[(t_{i+1} - t_i)\right]$$

where I is the instantaneous current at the time t in the series resistance R and V_T is the corresponding total voltage across the series combination of gap and resistor. The subscripts are used to designate the time increment boundaries.

The data reduction was accomplished using a Type 17A Universal Telereader (manufactured by Telecomputing Corporation, Burbank, California) and a counter from the Graphic Systems Division of Computer Industries Inc., Paramus, New Jersey. The relative values of current

and voltage were produced as a function of time on IBM punch cards. The following two computer programs were written to numerically reduce the data to current, voltage, power, and energy in the gap and to plot these values as a function of time.

a. Current in the series resistance and the total voltage across the series combination of gap and resistance.

```
      Program Spark (Input, Tapes = Input, Output, Tape 6 = Output)
      Dimension TC(100), TV(100), V(100), VNEW(100)
      Dimension C(100), VS(100), PTOT(100), PRES(100), PSPARK(100)
      Dimension Energy(100), Q(100), ERES(100), FRACTE(100)
C     Read in Next Data Deck
      Read (5,110) NRUN
  110 Format (I2)
      If (NRUN) 115,115,1
1     Continue
C     Read in Time Scale Per Division from Scope in Units of 10-6 Sec
   11 Read (5,25) CALT
   25 Format (F10.0)
C     Read in Current and Volts per Division (From Oscilloscope)
      Read (5,5) CALI, CALV
    5 Format (2F10.0)
C     Read in Data When Plotter is Moved One Large Division Vertically
      Read (5,10)     WNON,DIVI
   10 Format (F5.0,1X,F5.0)
```

```
C     Read in Data When Plotter is Moved One Large Division Horizontally
      Read (5,10) DIVT,WNO
C     Read in CIC and CC, Origin Correction for Current
      Read (5,10) CTC,CC
C     Read in CTV and CV, Origin Correction for Voltage
      Read (5,10) CTV,CV
C     Read in Number of Current Data Points
      Read (5,15) NI
   15 Format (I2)
C     Read in Number of Voltage Data Points
      Read (5,20) NV
   20 Format (I2)
C     Read in Value of Resistance, Capacitance, and Voltage
      Read (5,25) R
      Read (5,25) CAP
      Read (5,25) VOL
C     Read in Data; Current First
      Read (5,35) (TC(I),C(I),I=1,NI)
   35 Format ((6(F5.0,1X,F5.0,1X)))
      Print 38
   38 Format (16H New Page Please)
      Print 39
   39 Format (1H1)
      Read (5,40) (TV(I),V(I),I=1,NV)
```

```
40 Format ((6(F5.0,1X,F5.0,1X)))
   Print 24, NRUN
24 Format (15H Run Number is ,I2)
   Print 26,R
26 Format (39H the Value of the Resistance in Ohms is, F10.2)
   Print 27, CAP
27 Format (38H the Value of the Capacitance in PF is, F10.2)
   Print 28, VOL
28 Format (37H the Value of the Voltage in Volts is, F10.2)
   Print 29, CALI
29 Format (45H the Value of CALI, Current per Div in Amps is, F8.3)
   Print 30, CALV
30 Format (36H the Value of CALV, Volts per Div is, F8.2)
   Print 31, CALT
31 Format (47H the Value of Sweep Time per Div in 10-6 Sec is, F8.2)
   Print 99
99 Format (1H0)
   Print 200
200 Format (14H Current Data)
   Print 42, (C(I), I=1,NI)
42 Format (10F11.3)
   Print 99
   Print 210
```

```
210 Format (28H Voltage Data Across Total)
    Print 42, (V(I), I=1,NV)
    Print 99
    AMPDIV=(CALI/DIVI)
    VOTDIV=(CALV/DIVI)
    TDIV=(CALT/DIVT)
    DO 45 I=1,NI
    TC(I)=(TC(I)-CTC)*TDIV
 45 C(I)=(C(I)-CC)*AMPDIV
    Print 220
220 Format (17H Current in Amps)
    Print 43, (C(I),I=1,NI)
 43 Format (10F11.5)
    Print 99
    Print 225
225 Format (* Current Time in Microseconds*)
    Print 42, (TC(I),I=1,NI)
    Print 99
    DO 50 I=1,NV
    TV(I)=(TV(I)-CTV)*TDIV
 50 V(I)=(V(I)-CV)*VOTDIV
    Print 228
228 Format (* Voltage Time in Microseconds*)
    Print 42, (TV(I),I=1,NV)
```

```
      Print 99
      Print 230
230   Format (22H Voltage Across Total)
      Print 44, (V(I),I=1,NV)
 44   Format (10F10.2)
      Print 99
      DO 51 I=1,NI
      DO 52 K=1,NV
      J=K
      If (TV(K)-TC(I)) 52,52,53
 52   Continue
      Print 400
400   Format (* Last Voltage Time Taken Was Not Greater than the Last
      Current Time*)
      Stop
 53   If (J.EQ.1) go to 401
      VNEW(I)=V(J-1)+(V(J)-V(j-1))*(TC(I)-TV(J-1))/(TV(J)-TV(J-1))
 51   Continue
      Go to 404
401   Print 402
402   Format (* First Voltage Time Taken Was Greater Than First Current
      Time*)
      Stop
```

```
404 Continue
    Print 235
235 Format (26H New Voltage Across Total)
    Print 44, (VNEW(I),I=1,NI)
    Print 99
    DO 57 I=1,NI
 57 VS(I)=VNEW(I)-C(I)*R
    Print 250
250 Format (22H Voltage Across Spark)
    Print 44, (VS(I),I=1,NI)
    Print 99
    DO 60 I=1,NI
 60 PTOT(I)=VNEW(I)*C(I)
    Print 260
260 Format (22H Total Power in Watts)
    Print 42, (PTOT(I),I=1,NI)
    Print 99
    DO 65 I=1,NI
 65 PRES(I)=((C(I)**2))*R
    Print 270
270 Format (33H Power Across Resistor in Watts)
    Print 42, (PRES(I),I=1,NI)
    Print 99
    DO 68 I=1,NI
```

```
 68 PSPARK(I)=VS(I)*C(I)
    Print 280
280 Format (30H Power Across Spark in Watts)
    Print 42, (PSPARK(I),I=1,NI)
    Print 99
    M=NI 1
    DO 70 I=1,M
    L=I+1
    ERES(I)=((PRES(L)+PRES(I))*(TC(L)-TC(I)))*5.
 70 Energy(I)=((PSPARK(L)+PSPARK(I))*(TC(L)-TC(I)))*5.
    Print 290
290 Format (31H Spark Average Energy in Ergs)
    Print 42, (Energy(I),I=1,M)
    Print 99
    Print 295
295 Format (34H Resistor Average Energy in Ergs)
    Print 42, (ERES(I), I=1,M)
    Print 99
    ETOT=0.0
    DO 80 I=1,M
 80 ETOT=ETOT + Energy(I)
    ERTOT=0.0
    DO 85 I=1,M
 85 ERTOT=ERTOT + ERES(I)
```

```
      DO 90 J=1,M
      B=0.0
      DO 90 I=1,J
      B = Energy(I) + B
      FRACTE(J) = B
   90 Continue
      DO 95 J=1,M
   95 FRACTE(J)=(FRACTE(J)/ETOT)
      Print 300
  300 Format (1.. Fraction Energy)
      Print 42, (FRACTE(J),J=1,M)
      Print 99
      Write (6,100)ETOT
  100 Format (16H ETOTAL in Ergs, = F12.3)
      Print 99
      M=NI-1
      DO 101 I=1,M
      L=I+1
  101 Q(I)=((C(L)+C(I))*(TC(L)-TC(I)))/2.
      QTOT=0
      DO 102 I=1,M
      QTOT=QTOT+Q(I)
  102 Continue
      COULOM=QTOT*0.000001
```

```
      Write (6,103)COULOM
  103 Format (10H COULOMB=,E12.5)
      Print 99
      Write (6,104)ERTOT
  104 Format (34H Energy Across Resistor in Ergs=,F12.3)
      DO 105 I=1,NI
  105 TC(I)=I-1
      Call Nancy (TC,C,NI,0,0,0,0,2,1)
      Call Label (4HTIME,10H(MICROSEC),7HCURRENT,9H(AMPERES),NRUN)
      Call Nancy (TC,VNEW,NI,0,0,0,0,2,1)
      Call Label (4HTIME,10H(MICROSEC),7HVOLTAGE,7H(VOLTS),NRUN)
      Call Nancy (TC,VS,NI,0,0,0,0,2,1)
      Call Label (4HTIME,10H(MICROSEC),6HVSPARK,7H(VOLTS),NRUN)
      Call Nancy (TC,PSPARK,NI,0,0,0,0,2,1)
      Call Label (4HTIME,10H(MICROSEC),6HPSPARK,7H(WATTS),NRUN)
      Call Nancy (TC,Energy,M,0,0,0,0,2,1)
      Call Label (4HTIME,10H(MICROSEC),10HENERGYSPRK,6H(ERGS),NRUN)
      Call Nancy (TC,FRACTE,M,0,0,0,0,2,1)
      Call Label (4HTIME,10H(MICROSEC),8HFRACTION,1H ,NRUN)
      Call Nancy (VS,C,NI,0,0,0,0,2,1)
      Call Label (6HVSPARK,7H(VOLTS),7HCURRENT,9H(AMPERES),NRUN)
      Call Nancy (TC,Q,M,0,0,0,0,2,1)
      Call Label (4HTIME,10H(MICROSEC),8HCOULOMBS,7H(10-6C),NRUN)
      Read (5,110) NRUN
```

```
      If (NRUN) 115,115,11
  115 Continue
      End
```

b. Voltage across the series resistance and the total voltage across the series combination of gap and resistance.

```
      Program Spark (Input, Tapes = Input, Output, Tape 6 = Output)
      Dimension TVR(100), TVT(100), VR(100), VT(100)
      Dimension C(100), VS(100), PTOT(100), PRES(100)
      Dimension PSPARK(100), Energy(100), VNEW(100), Q(100)
      Dimension FRACTE(100), ERES(100)
      Dimension TV(100), TC(100)
      Equivalence (TV(1), TVT(1)), (TVR(1), TC(1))
C     Read in Next Data Deck
      Read (5,110) NRUN
  110 Format (I2)
      IF (NRUN) 115,115,1
    1 Continue
C     Read in Time Scale Per Division from Scope in Units of 10-6 Sec
   11 Read (5,25) CALT
   25 Format (F10.0)
C     Read in Volts Resistor and Volts Total Per Division, From Scope
      Read (5,5) CALVR, CALVT
    5 Format (2F10.0)
```

```
C     Read in Data When Plotter Is Moved One Large Division Vertically
      Read (5,10) WNON, DIVV
   10 Format (5.0,1X,F5.0)
C     Read in Data When Plotter Is Moved One Large Division Horizontally
      Read (5,10) DIVT, WNO
C     Read in CTVR and CVR, Origin Correction for Volts Across Resistor
      Read (5,10) CTVR, CVR
C     Read in CTVT and CVT, Origin Correction for Volts Across Total
      Read (5,10) CTVT, CVT
C     Read in Number of Data Points for Volts Across Resistor
      Read (5,15) NR
   15 Format (I2)
C     Read in Number of Data Points for Volts Across Total
      Read (5,20) NV
   20 Format (I2)
C     Read in Value of Resistance, Capacitance, and Voltage
      Read (5,25) R
      Read (5,25) CAP
      Read (5,25) VOL
C     Read in Data, Volts Across Resistor First
      Read (5,35) (TVR(I),VR(I),I=1,NR)
   35 Format ((6(F5.0,1X,F5.0,1X)))
      Print 38
```

```
38 Format (16H New Page Please)
   Print 39
39 Format (1H1)
   Read (5,40) (TVT(I),VT(I),I=1,NV)
40 Format ((6(F5.0,1X,F5.0,1X)))
   Print 24, NRUN
24 Format (15H Run Number Is I2)
   Print 26 R
26 Format (39H the Value of the Resistance in Ohms Is,F10.2)
   Print 27, CAP
27 Format (38H the Value of the Capacitance in pF Is,F10.2)
   Print 28, VOL
28 Format (37H the Value of the Voltage in Volts Is,F10.2)
   Print 29, CALVR
29 Format (45H the Value of CALVR, Volts Across R Per Div Is,F8.2)
   Print 30, CALVT
30 Format (49H the Value of CALVT, Volts Across Total Per Div Is,F8.2)
   Print 31, CALT
31 Format (47H the Value of Sweep Time Per Div in 10-6 Sec Is,F8.2)
   Print 99
49 Format (1H0)
   Print 200
200 Format (30H Voltage Data Across Resistor)
   Print 42, (VR(I),I=1,NR)
```

```
 42 Format (10F11.3)
    Print 99
    Print 210
210 Format (28H Voltage Data Across Total)
    Print 42, (VT(I),I=1,NV)
    Print 99
    VORDIV=(CALVR/DIVV)
    VOTDIV=(CALVT/DIVV)
    TDIV=(CALT/DIVT)
    DO 45 I=1,NR
    TVR(I)=(TVR(I)-CTVR)*TDIV
 45 VR(I)=(VR(I)-CVR)*VORDIV
    Print 220
220 Format (25H Voltage Across Resistor)
    Print 44, (VR(I),I=1,NR)
 44 Format (10F10.2)
    Print 99
    DO 50 I=1,NV
    TVT(I)=(TVT(I)-CTVT)*TDIV
 50 VT(I)=(VT(I)-CVT)*VOTDIV
    Print 225
225 Format (* Time Volts Across Resistor in Microseconds*)
    Print 42, (TVR(I),I=1,NR)
    Print 99
```

```
      Print 230
  230 Format (22H Voltage Across Total)
      Print 44, (VT(I), I=1,NV)
      Print 99
      Print 228
  228 Format (* Total Voltage Time in Microseconds*)
      Print 42, (TVT(I),I=1,NV)
      Print 99
      DO 55  I=1,NR
   55 C(I)=VR(I)/R
      Print 240
  240 Format (17H Current in Amps)
      Print 43, (C(I), I=1,NR)
   43 Format (10F11.5)
      Print 99
      DO 51 I=1,NR
      DO 52 K=1,NV
      J=K
      IF (TV(K)-TC(I)) 52,52,53
   52 Continue
      Print 400
  400 Format (* Last Voltage Time Taken Was Not Greater Than the Last
      Current Time*)
      Stop
```

```
 53 IF (J.EQ.1) go to 401
    VNEW(I)=VT(J-1)+(VT(J)-VT(J-1))*(TC(I)-TV(J-1))/(TV(J)-TV(J-1))
 51 Continue
    Go to 404
401 Print 402
402 Format (* First Voltage Time Taken Was Greater Than First Current
    Time*)
    Stop
404 Continue
    Print 235
235 Format (26H New Voltage Across Total)
    Print 44, (VNEW(I), I=1, NR)
    Print 99
    DO 57 I=1, NR
 57 VS(I)=VNEW(I)-VR(I)
    Print 250
250 Format (22H Voltage Across Spark)
    Print 44, (VS(I),I=1,NR)
    Print 99
    DO 60 I-1,NR
 60 PTOT(I)=VNEW(I)*C(I)
    Print 260
260 Format (22H Total Power in Watts)
    Print 42, (PTOT(I),I=1,NR)
```

```
      Print 99
      DO 65 I=1,NR
   65 PRES(I)=VR(I)*C(I)
      Print 270
  270 Format (33H Power Across Resistor in Watts)
      Print 42, (PRES(I),I=1,NR)
      Print 99
      DO 68 I=1,NR
   68 PSPARK(I)=VS(I)*C(I)
      Print 280
  280 Format (30H Power Across Spark in Watts)
      Print 42, (PSPARK(I),I=1,NR)
      Print 99
      M=NR-1
      DO 70 I=1,M
      L=I+1
      ERES(I)=((PRES(L)+PRES(I))*(TVR(L)-TVR(I)))*5.
   70 Energy(I)=((PSPARK(L)+PSPARK(I))*(TVR(L)-TVR(I)))*5.
      Print 290
  290 Format (31H Spark Average Energy in Ergs)
      Print 42, (Energy(I),I=1,M)
      Print 99
      Print 295
```

```
295 Format (34H Resistor Average Energy in Ergs)
    Print 42, (ERES(I),I=1,M)
    Print 99
    ETOT=0.0
    DO 80 I=1,M
 80 ETOT=ETOT+Energy(I)
    ERTOT=0.0
    DO 85 I=1,M
 85 ERTOT=ERTOT+ERES(I)
    DO 90 J=1,M
    B=0.0
    DO 90 I=1,J
    B=Energy(I) + B
    FRACTE(J) = B
 90 Continue
    DO 95 J=1,M
 95 FRACTE(J)=(FRACTE(J)/ETOT)
    Print 300
300 Format (17H Fraction Energy)
    Print 42, (FRACTE(J),J=1,M)
    Print 99
    Write (6,100)ETOT
100 Format (16H ETOTAL in Ergs=,F12.3)
    Print 99
```

```
      M=NR-1
      DO 101 I=1,M
      L=I+1
101   Q(I)=((C(L)+C(I))*(TVR(L)-TVR(I)))/2.
      QTOT=0
      DO 102 I=1,M
      QTOT=QTOT+Q(I)
102   Continue
      COULOM=QTOT*0.000001
      Write (6,103)COULOM
103   Format (10H COULOMB=,E12.5)
      Print 99
      Write (6,104)ERTOT
104   Format (34H Energy Across Resistor in Ergs=,F12.3)
      DO 105 I=1,NR
105   TVR(I)=I-1
      Call Nancy (TVR,VR,NR,0,0,0,0,2,1)
      Call Label (4HTIME,10H(10-6 Sec), 7HVRESIST,7H(Volts),NRUN)
      Call Nancy (TVR,VNEW,NR,0,0,0,0,2,1)
      Call Label (4HTIME,10H(10-6 Sec),6HVTOTAL,7H(Volts),NRUN)
      Call Nancy (TVR,C,NR,0,0,0,0,2,1)
      Call Label (4HTIME,10H(10-6 Sec),7HCURRENT,9H(Amperes),NRUN)
      Call Nancy (TVR,VS,NR,0,0,0,0,2,1)
      Call Label (4HTIME,10H(10-6 Sec),6HVSPARK,7H(Volts),NRUN)
```

```
      Call Nancy (TVR,PSPARK,NR,0,0,0,0,2,1)
      Call Label (4HTIME,10H(10-6 Sec),6HPSPARK,7H(Watts),NRUN)
      Call Nancy (TVR,Energy,M,0,0,0,0,2,1)
      Call Label (4HTIME,10H(10-6 Sec),10HENERGYSPRK,6H(Ergs),NRUN)
      Call Nancy (TVR,FRACTE,M,0,0,0,0,2,1)
      Call Label (4HTIME,10H(10-6 Sec),8HFRACTION,1H ,NRUN)
      Call Nancy (VS,C,NR,0,0,0,0,2,1)
      Call Label (6HVSPARK,7H(Volts),7HCURRENT,9H(Amperes),NRUN)
      Call Nancy (TVR,Q,M,0,0,0,0,2,1)
      Call Label (4HTIME,10H(10-6 Sec),8HCOULOMBS,8H(10+6C),NRUN)
      Read (5,110)NRUN
      IF (NRUN) 115,115,11
  115 Continue
      End
```